Pakistan Veterinary Journal

ISSN: 0253-8318 (PRINT), 2074-7764 (ONLINE)
DOI: 10.29261/pakvetj/2026.099

RESEARCH ARTICLE

Mining Anti-Infectious Bronchitis Virus Medication Rules and Verifying Formula Efficacy via the TCM Inheritance Computing Platform

Huixin Liu[1,2], Xiaofang Wei[2], Sijia Pan[2], Chenchen Wang[2], Weiwu Mu[2,5], Maha Abdullah Momenah[3], Yasser S. Mostafa[4], Fanan Suksawat[5], Hongbin Si[2], Liangyu Yang[1*] and Bin Xiang[1*]

[1]College of Veterinary Medicine, Yunnan Agricultural University, Kunming, Yunnan 650201, China; [2]College of Animal Science and Technology, Guangxi University, Nanning, 530004, Guangxi, China; [3]Department of Biology, College of Science, Princess Nourah bint Abdulrahman University, P.O. Box 84428, Riyadh 11671, Saudi Arabia; [4]Department of Biology, College of Science, King Khalid University, Abha, P.O. Box 9004, Saudi Arabia; [5]Faculty of Veterinary Medicine, Khon Kaen University,Khon Kaen 40002, Thailand.
*Corresponding author: xiangbin2018@126.com

ARTICLE HISTORY (26-415)

Received:	April 15, 2026
Revised:	May 16, 2026
Accepted:	May 19, 2026
Published online:	May 22, 2026

Key words:
Anti-inflammation
Antioxidation
Immunomodulation
Infectious bronchitis virus (IBV)
TCM Inheritance Computing Platform
Traditional Chinese Medicine

A B S T R A C T

Avian infectious bronchitis virus (IBV) is a highly infectious pathogen, which seriously threatens the global poultry industry. Traditional Chinese Medicine (TCM) has shown some potential in the fight against IBV infection, but its application in the veterinary field is limited by the lack of systematic and massive data support. Based on the TCM inheritance computing platform, this study integrated 34,324 TCM prescriptions, 7,505 Chinese patent medicines and 4,207 platform-specific formulas, screened 336 candidate formulas consistent with IBV clinical phenotypes and obtained 5 core formulas through association rule and clustering analyses. The therapeutic effects of the IBV-infected yellow-feathered broilers were evaluated. The TCM compound had time- and group-dependent anti-IBV effects. TCM-1 performed the best in alleviating clinical symptoms and restoring growth; TCM-1/2/5 alleviated symptoms on the 14th day and TCM-2/3 significantly promoted weight gain. These formulations protected the thymus and bursa of Fabricius but did not affect the spleen index. Different formulations reduced the viral load in a time- and tissue-dependent manner. TCM-2/3 significantly increased antibody levels, and all formulations balanced inflammatory cytokines and oxidative stress better than ribavirin. TCM-5 showed the best tracheal ciliary protection effect, while TCM-4 had the poorest overall efficacy. This study identified the TCM formula pattern for IBV using a data-mining approach previously established in human medicine and verified their therapeutic potential in a chicken model. The observed effects were associated with immunomodulation, antioxidation, and anti-inflammation. Although the methodology is not entirely novel in human TCM, its application to avian IBV with multi-dimensional *in-vivo* validation represents an advance in veterinary phytomedicine. This study provides evidence-based candidates for the clinical prevention and treatment of infectious bronchitis in chickens. This study provides evidence-based candidates for the clinical prevention and treatment of infectious bronchitis in chickens.

To Cite This Article: Liu H, Wei X, Pan S, Wang C, Mu W, Momenah MA, Mostafa YS, Suksawat F, Si H, Yang L and Xiang B, 2026. Mining anti-infectious bronchitis virus medication rules and verifying formula efficacy via the tcm inheritance computing platform. Pak Vet J, 46(5): 1092-1109. http://dx.doi.org/10.29261/pakvetj/2026.099

INTRODUCTION

Avian infectious bronchitis (IB) is an acute and highly contagious respiratory disease in chickens caused by the infectious bronchitis virus (IBV), this virus belongs to the *γ-coronavirus* genus of the *Nidovirales* order and the *Coronaviridae* family (Jing *et al*., 2025). The characteristic of IBV is its significant variability and the existence of multiple serotypes, which poses considerable challenges to immune control and prevention (Huang *et al*., 2025). The typical symptoms of this disease include tracheitis, conjunctivitis and ciliary stasis. It can affect chickens of different breeds and ages (Jackwood *et al*., 2015). Clinically, IBV infection manifests as respiratory

symptoms and systemic signs, such as weight gain or loss, reduced egg production, decreased eggshell quality, and lower feed conversion efficiency. It can also lead to problems like pseudoeggs and secondary bacterial infections, imposing a significant economic burden on the global poultry industry (Zhang *et al*., 2020; Quinteros *et al*., 2022).

Due to the high variability of the IBV strain, immune failure is a common phenomenon, which further complicates the prevention and control efforts (Legnardi *et al*., 2020). In China, the government has prohibited the use of antiviral drugs in food animals to control drug residue, which presents a new challenge for IBV management (Sasse *et al*., 2024). At the same time, the use of traditional Chinese medicine (TCM) in the treatment of IBV has gained increasing attention (Abbas *et al*., 2022; Xiang *et al*., 2026). TCM offers unique advantages in regulating the physiological functions of animals, enhancing immunity, and improving disease resistance and antiviral capabilities (Prajapati *et al*., 2022; Lu *et al*., 2024; Yu *et al*., 2025). Moreover, TCM's integrative approach can effectively complement the shortcomings of modern drug treatments. The exploration and application of antiviral compound TCM formulations may become an alternative or supplementary strategy to IBV vaccination (Gul *et al*., 2023).

The TCM Inheritance Computing Platform is an auxiliary system for the inheritance and research and development of TCM, constructed based on big data mining and intelligent analysis technologies (Ren *et al*., 2023). Its core functions encompass the integration and processing of vast amounts of TCM prescription and medical case data, as well as the integrated application of data mining algorithms such as association rule analysis and cluster analysis (Chen & He, 2022; Zhang, Hou, *et al*., 2022; Zhao *et al*., 2022). This platform can explore the functionalities and applications of TCM diagnostic rules, characteristics of prescription compatibility, the construction of intelligent experience inheritance systems in TCM, and the computational system for the inheritance of TCM, thus providing technical support for the inheritance of TCM theory and the optimization of clinical diagnosis and treatment (Liu *et al*., 2022). Initially, it was used for the mining and optimization of human TCM prescriptions. TCM diagnosis is a crucial component of TCM; it is a method for understanding patients' conditions, analyzing illnesses, and differentiating syndromes to guide treatment (Tian *et al*., 2024). Animals cannot express their symptoms directly like humans; however, their pathological states can be analogous to those of humans. Therefore, the application of TCM in the treatment of animal diseases often requires reference to treatment methods for similar symptoms in humans (Wang *et al*., 2023; Wang, *et al*., 2025). Additionally, many drugs are validated using animals as experimental models before they are marketed (Polis & Samson, 2024).

According to the theory of TCM, infectious bronchitis in chickens is classified as wind-warm syndrome of the Qi-blood blazing type. During the onset of the disease, chickens kept in enclosed and poorly ventilated environments for extended periods are vulnerable to attack by external pathogenic factors, particularly wind pathogen and heat pathogen (Liu *et al*., 2025). After invading the body through the respiratory tract, these pathogenic factors first impair the lung meridian, leading to failure of lung qi to disperse, and then symptoms such as cough, chest distress, sore throat and swollen uvula arise (Ichikawa *et al*., 2013). In traditional Chinese veterinary medicine (TCVM), the therapeutic principles for treating IBV usually include clearing heat and detoxification, resolving phlegm, relieving cough and asthma. Existing studies have confirmed that several herbal medicines exhibit certain therapeutic effects against IBV, including *Hypericum perforatum* (Chen *et al*., 2019), *Allium sativum* (Mohajer Shojai *et al*., 2016), *Sambucus nigra* (Chen *et al*., 2014) and Shegandilong granule (SGDL) (Feng *et al*., 2021).

The TCM inheritance computing platform was originally developed for human prescription analysis. However, its use in IBV can be justified. First, IBV infection in chickens causes respiratory mucosal damage, cough, phlegm, and systemic inflammation. These features are similar to a common human TCM pattern known as wind-warm pathogen attacking the lung with phlegm-heat stagnation. Second, IBV belongs to the Coronaviridae family and shares genomic and pathogenic traits with human coronaviruses such as SARS-CoV-2. Several herbs identified in this study, including *Glycyrrhiza uralensis*, *Ephedra sinica* and *Scutellaria baicalensis*, have been reported to show antiviral activity against human coronaviruses. Based on these considerations, this study applies the platform to identify potential anti-IBV herbal combinations and validates their efficacy *in-vivo*. The goal is to provide new therapeutic options for IBV control and to offer a theoretical basis for the rational application of veterinary TCM.

MATERIALS AND METHODS

TCM prescription mining study: Source of Prescriptions: Through cross-retrieval of 34,324 TCM (TCM) formula datasets from the China Formula Database, 7,505 TCM patent medicine formulation datasets from the Cross-retrieval Database of Traditional Chinese Patent Medicine Formulas, 33,837 traditional formula records, 4,207 TCM patent medicine formulation datasets from the TCM Inheritance Computing Platform, as well as the Chinese Veterinary Pharmacopoeia, with keywords including "cough", "lung", "toxin" and "phlegm", a total of 1,121 accurately recorded TCM formulas from the China Formula Database, 853 Chinese patent medicine entries and 1,102 traditional formula records from the Cross-retrieval Database of Traditional Chinese Patent Medicine Formulas, 464 patent formulations from the 4,207 TCM patent medicine formulation datasets of the TCM Inheritance Computing Platform, 11 patent formulations from the Chinese Veterinary Pharmacopoeia, and 11 formulas of new veterinary drugs were obtained.

Prescription Selection Criteria: Three veterinary medicine researchers were assigned to conduct data collation of the collected formulas. Only those existing patent formulas consistent with the pathogenesis of IBV infection in chickens were included for subsequent

analysis. In addition, duplicate formulas with identical herbal compositions were merged; non-pure TCM preparations were excluded. For the formulas retrieved using the keyword "cough", those associated with TCM diseases that induce cough but are irrelevant to IBV infection - such as trachoma, toothache, acute epidemic conjunctivitis, and dysmenorrhea - were also eliminated. Herbal processing methods were not considered temporarily, and all medicinal materials were counted based on their raw forms. The final valid dataset was determined by taking the intersection of the data independently collated by the three researchers.

Data Analysis: Data were analyzed using the "TCM Inheritance Computing Platform V3.0" software. The "Data Analysis" module was used to perform statistical and mining analyses, including "Statistical Analysis," "Prescription Analysis," and "Symptom Analysis." The frequency of medicinal ingredients, their properties (such as "Four Natures" and "Five Flavors"), medicinal effects, and meridian tropism were statistically analyzed. In TCM, medicinal ingredients are classified based on their "Four Natures" (the four temperature qualities: cold, cool, warm, hot) and "Five Flavors" (the five tastes: sweet, sour, bitter, pungent, salty). These qualities help to determine the therapeutic effect of the medicine on the body. "Meridian tropism" refers to the specific pathways or meridians in the body that a herb targets, influencing its action on different organ systems. Symptom patterns and prescription formulations were further analyzed using association rules and k-means clustering (Zhu *et al*., 2021). In the association rules analysis, a support value of 25 and a confidence value of 0.7 were applied to examine the correlations between drugs. In the clustering analysis, the number of clusters was set to k=5, which was determined based on the elbow method of within-cluster sum of squares and the clinical interpretability of the resulting herb combinations. Each cluster represents a distinct compatibility pattern. The centroid formula of each cluster was selected for subsequent *in-vivo* testing.

Reagents and Animals

Viral strain: The pathogenic IBV strain M41 (batch number AV1511) was purchased from the China Veterinary Drug Inspection Institute. The strain was propagated in 10-day-old specific pathogen-free (SPF) chicken embryos (Guangxi Veterinary Research Institute). A 100 μL aliquot of the IBV M41 strain was inoculated into the SPF chicken embryos under sterile conditions. The survival status of the embryos was observed every 12 hours, and any embryos that died within 24 hours were discarded. After 72 hours post-inoculation, allantoic fluid was collected from the infected embryos and stored at -80°C. The 50% embryo infectious dose (EID_{50}) of the IBV M41 strain in SPF chicken embryos was determined and calculated using the Reed-Muench method.

Herbal medicines: The herbal medicines used in this study were purchased according to the prescription formulas developed for the experiment, with the drugs provided by Xiangxiang Pharmacy in Guangxi Province, China. The five TCM compound extracts were prepared by decoction, with the herbs mixed in a 1:1 ratio. This equal-ratio approach is a common initial screening strategy when the active components and their optimal proportions are unknown; it allows for unbiased assessment of whether a given formula concept exhibits biological activity. Optimization of herb ratios is reserved for subsequent studies. This ratio was chosen to assess whether the herbal combination would produce a certain effect, without prior determination of the active ingredients or their specific therapeutic properties. The mixed medicinal materials were soaked in cold water to submerge their surface for 30 minutes, then boiled over high heat before switching to low heat for another 30 minutes, after which the decoction was poured out. The herbal residues were re-boiled twice with fresh water following the identical procedure as the first extraction. The three batches of decoction were combined, filtered to remove the herbal residues, and the supernatant was collected. The supernatant was concentrated on a concentration of 1 g/mL using a vacuum pump and a rotary evaporator under the conditions of 0.08 MPa and 60°C and then stored for subsequent use (Zhang *et al*., 2017). Yellow-feathered broiler chicks were purchased from Guangxi Fufeng Animal Husbandry Group Co., Ltd. (Nanning, Guangxi, China). The chicks were housed in wire cages with adequate ventilation and lighting and had ad libitum access to feed and water throughout the experiment. At 14 days of age, the chicks were randomly assigned into 8 groups using a random number table, with 20 chicks per group. Randomization was performed before any treatment. The groups were designated as follows: blank control group (NC), TCM formula 1-5 treatment groups (TCM-1 to TCM-5, each at 1 mL/0.5 L), positive drug control group (ribavirin, 100 mg/0.5 L) and IBV model group (IBV). The NC and IBV groups were administered physiological saline as the control. The investigator responsible for clinical scoring and sample collection was blinded to group allocation. However, due to the distinct appearance and odor of the TCM decoctions, blinding during drug administration was not feasible. The experiment was initiated 14 days of age, with continuous administration of the corresponding treatments for 1 week and the entire experimental period lasted 14 days. On the same day of viral challenge, the treatment groups received the respective TCM formulas. All groups except the NC group were challenged via the intranasal and intraocular routes with IBV at a dose of 10^5 EID_{50}. All chicks were then housed in molded plastic isolation units and provided with free access to feed and water.

Animals: From 14 days of age, the treatment groups received their respective TCM compounds for 7 consecutive days. The experiment lasted for a total of 14 days. On the day of the viral challenge, all groups except the blank control group were inoculated intranasally and ocularly with IBV at a dose of 10^5 EID_{50}. All chicks were housed in plastic separation enclosures and were allowed free access to food and water throughout the experiment. The animal experiments were approved by the Animal Protection and Welfare Committee of Guangxi University (approval number GXU-2021-105) and were conducted in accordance with the ethical guidelines and approved protocols. All procedures followed the ARRIVE guidelines (https://arriveguidelines.org).

Comparison of therapeutic effects in animal experiment

Efficacy evaluation and daily weight gain: All chicks were housed in molded plastic separate enclosures and were allowed free access to food and water. After the infection, five chicks from each group were randomly selected and observed for 14 days. The growth efficiency was measured by monitoring their weight and clinical signs. The clinical signs were assessed according to the scoring criteria in Table 1, including mental state, feeding and drinking behavior, head shaking, wheezing, sneezing, and coughing.

Table 1: Chick clinical symptom scoring criteria

Curative effect	Clinlcal symptom	value
Death	The dead chickens were found to have died of infectious bronchitis after necropsy and PCR testing.	5
Invalid	Chickens may exhibit symptoms of depression such as lying down, rough feathers, closed eyes, lethargy, reduced food consumption, neck stretching, severe rales, visible mucus in the mouth and nose, coughing, and white or watery diarrhea.	4
Somewhat relieved	The chicken displays signs of low energy, reluctance to exercise, decreased appetite, a slight cough, abnormal breath sounds (rales), presence of mucus in the mouth and nasal cavity, and mild diarrhea.	3
moderately relieved	The chicken is in a good mental state, occasionally exercises, has a decreased appetite, breathes through the mouth, and has mucus in the mouth.	2
considerably relieved	The chickens exhibit signs of good mental well-being, with normal breathing and appetite. Some chickens may display mouth breathing and have a slight presence of mucus in their mouths.	1
completely relieved	The chicken is in good spirits and its breathing and appetite have returned to normal.	0

Immune organ indices: At 3, 7 and 14 days post-infection (dpi), five chicks from each group were randomly selected for weight measurement. Collect the spleens, thymuses and bursa of Fabricius from each group, weigh them separately, and calculate the relative organ weights as the immune organ index. The calculation of the immune organ index is as follows: Immune organ index=organ weight (mg) / body weight (g).

Detection of viral load and antibody levels: Samples were collected on the 3rd, 7th and 14th days. Five chicks were randomly selected from each group and euthanized by cervical dislocation. The tracheal tissues were immediately harvested and placed in sterile centrifuge tubes for subsequent analysis. For serum preparation, the blood samples were left at room temperature for 2 hours, then centrifuged at 3,000 rpm for 10 minutes to separate the serum; the resulting serum samples were stored at -80°C until further testing. The viral load in the trachea was quantified using quantitative real-time polymerase chain reaction (qPCR). According to the manufacturer's instructions, total viral RNA was extracted from the tracheal tissue homogenate using a column-based viral RNA extraction kit (Genstar). The extracted RNA was reverse-transcribed into complementary DNA (cDNA) using a reverse transcription kit (Genstar). qPCR amplification was performed using specific primers for IBV on a real-time fluorescence quantitative PCR instrument. The reaction system and cycling conditions were set according to the kit protocol, and the viral load was calculated using the 2^(-ΔΔCt) method. Serum levels of IBV-specific antibodies were determined by indirect enzyme-linked immunosorbent assay (ELISA) using a commercial kit (IDEXX Laboratories, Inc., Westbrook, ME, USA). All procedures were carried out in compliance with the manufacturer's standard protocols. The absorbance value at 450 nm was measured using a microplate reader, and antibody concentrations were calculated based on the standard curve generated from the kit's reference standards.

Serum oxidative stress indices in TCM-treated IBV chicks: Serum samples collected at 3, 7and 14 dpi as described in 3.3.4 were used for the detection of oxidative stress-related indices. The concentrations of nitric oxide (NO), malondialdehyde (MDA), xanthine oxidase (XOD) and the activity of ttotal antioxidant capacity (T-AOC) were measured using commercial biochemical reagent kits (Solarbio Beijing China). All detection procedures were performed following the manufacturer's instructions. A spectrophotometer was used to measure the absorbance values at the corresponding wavelengths, and the levels or activities of each index were calculated according to the standard curves and formulae provided in the kits.

Serum inflammatory cytokines in TCM-treated IBV chicks: Serum samples collected at 3, 7, and 14 dpi were used to quantify the concentrations of six inflammatory cytokines, namely interleukin-4 (IL-4), tumor necrosis factor-α (TNF-α), interferon-γ (IFN-γ), interleukin-10 (IL-10), interleukin-6 (IL-6), and interleukin-1β (IL-1β). Commercial ELISA kits specific for chicken cytokines (Beyotime Institute of Biotechnology, Nanjing, China) were employed for detection. All experimental procedures were performed strictly following the manufacturer's standard protocols. The optical density (OD) value at 450 nm was measured using a microplate reader, and the cytokine concentrations were calculated based on the standard curves provided with the kits.

SEM analysis of tracheal ciliary damage: At 7 dpi five chicks were randomly selected from each group and euthanized. The middle segment of the trachea was collected and cut into 0.5 cm long tissue pieces. The tissue samples were immediately fixed in 2.5% glutaraldehyde solution at 4°C for 24 h. After fixation the samples were rinsed three times with 0.1 mol/L phosphate-buffered saline PBS each for 15 min. Gradient dehydration was performed using 30, 50, 70, 80, 90, 95 and 100% ethanol each for 15 min. The dehydrated samples were dried by critical point drying with liquid carbon dioxide. The dried samples were mounted on sample stages and sputter-coated with gold. The tracheal ciliary ultrastructure was observed and imaged using a scanning electron microscope at an accelerating voltage of 10 kV. The arrangement density integrity of cilia and the morphological changes of the tracheal surface were observed and recorded.

Lung histopathological observation: At 7 dpi five chicks were randomly selected from each group for euthanasia. Lung tissue samples were collected and fixed in 4% paraformaldehyde solution at room temperature for 24 h. Fixed samples were dehydrated through a gradient of ethanol cleared with xylene and embedded in paraffin. Paraffin sections with a thickness of 5 μm were prepared using a microtome. The sections were dewaxed to water stained with hematoxylin and eosin HE and then dehydrated cleared and mounted with neutral balsam. The pathological changes of lung tissues were observed under an optical microscope. The morphological structures of primary bronchi parabronchi and respiratory capillaries were examined. The presence of pathological lesions such as hemorrhage congestion edema and necrotic cell debris was recorded and analyzed.

Statistical analysis: Sample size was estimated based on a preliminary power analysis (α=0.05, power=0.8, expected 30% difference in viral load), requiring a minimum of 4 chicks per group per time point. Accounting for potential mortality, 5 chicks per group per time point were used (n=5, total 20 per group at start). Data are presented as mean ± SEM. Comparisons between each treatment group and the IBV model group were performed using one-way ANOVA with Dunnett's post hoc test. Two-way ANOVA was used for time-dependent analyses. All tests were two-sided, and $P < 0.05$ was considered significant. No adjustment was made for multiple comparisons across different parameters or time points. Statistical analyses were performed using GraphPad Prism 9.0.

RESULTS

Data screening and database construction: Through a standardized screening process, 336 herbal prescriptions containing 361 different drug components were systematically identified for the treatment of IBV (Suppliementary materials 1). The established database comprehensively documents clinical manifestations associated with each prescription, with symptom distribution patterns (Fig. 1).

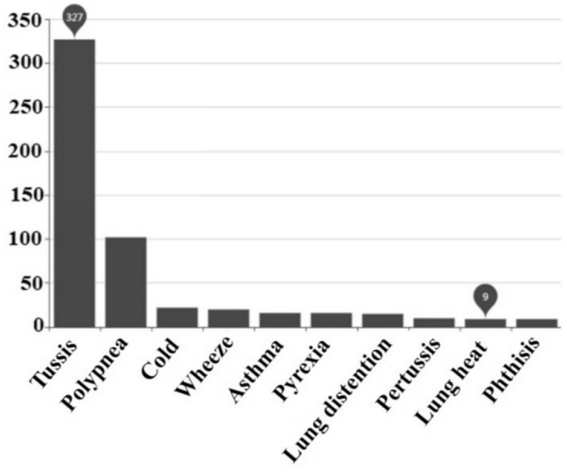

Fig. 1: Distribution of TCM diseases in the square (frequency greater than 9).

Prescription pattern characterization: Phytochemical analysis revealed different treatment preferences. Four properties: mainly warm medicinal ingredients (42.3%), followed by neutral (28.1%) and cold (19.6%) components; five flavors: sweet ingredients accounted for 38.7% of the formula, along with pungent (29.2%) and bitter (22.1%) components; meridians: the spleen meridian was the main one (34.5%), followed by the stomach meridian (27.8%) and the lung meridian (22.6%); pharmacological effects: the first item accounted for 41.2% of the total components, followed by the second item (23.8%) and the third item (18.3%) of the drugs (Table 2-4, Fig. 2A-C). The pharmacological effect chart (Fig. 2D) illustrates the various therapeutic effects of the herbs, with each numbered item representing a unique action. The first item, relieving cough, expectorating phlegm, and relieving asthma, refers to herbs that help control coughing, remove phlegm, and alleviate asthma or wheezing symptoms. The second item, clearing heat, describes herbs used to eliminate excessive internal heat, typically for fever, inflammation, or infection. The third item, tonifying essence, refers to drugs that can strengthen the body when qi, yin, or yang are insufficient. The fourth item, dispelling exterior pathogenic factors, involves herbs that drive out wind, cold, and heat, often used in the early stages of colds or flu. The fifth item, regulating qi, includes herbs that promote the smooth flow of qi (important energy) within the body, helping to alleviate symptoms caused by qi stagnation, such as abdominal distension, fullness, or pain. The sixth item, consolidating (consolidating) function, refers to herbs that help the body retain body fluids, especially in cases of excessive sweating or diarrhea. The seventh item, diuretic and dampness-eliminating, describes herbs that promote urination and help eliminate dampness within the body, useful for edema, urinary problems, or heaviness. The eighth item, calming the liver and extinguishing wind, involves herbs that calm the liver and extinguish wind, causing symptoms such as dizziness, tremors, or convulsions. The ninth item, calming the mind, refers to herbs that help soothe the mind and spirit, used to treat anxiety, insomnia, or emotional agitation. Finally, the tenth item, aiding digestion, includes herbs to improve digestion and alleviate symptoms such as abdominal distension, indigestion, or food stagnation.

Table 2: Analysis of the four Natures and five flavor

NO.	Four Natures	Frequency	Rate	NO.	Five Tastes	Frequency	Rate
1	Warm	1036	37.84%	1	Bitter	1593	37.12%
2	Cold	983	35.90%	2	Punfent	1272	29.64%
3	Neutral herbs	553	20.20%	3	Sweet	1139	26.54%
4	Cool	133	4.86%	4	Sour	168	3.91%
5	Hot	33	1.21%	5	Salty	119	2.77%

Table 3: Analysis of the meridian tropism

NO.	Meridian tropism	Frequency	Rate	NO.	Meridian tropism	Frequency	Rate
1	Lung	2286	34.55%	7	Large Intestine	387	5.85%
2	Spleen	965	14.58%	8	Bladder	186	2.81%
3	Stomach	916	13.84%	9	Gallbladder	137	2.07%
4	Heart	685	10.35%	10	Small Intestine	100	1.51%
5	Liver	470	7.10%	11	Triple Burner	26	0.39%
6	Kidney	449	6.78%	12	Pericardium	12	0.18%

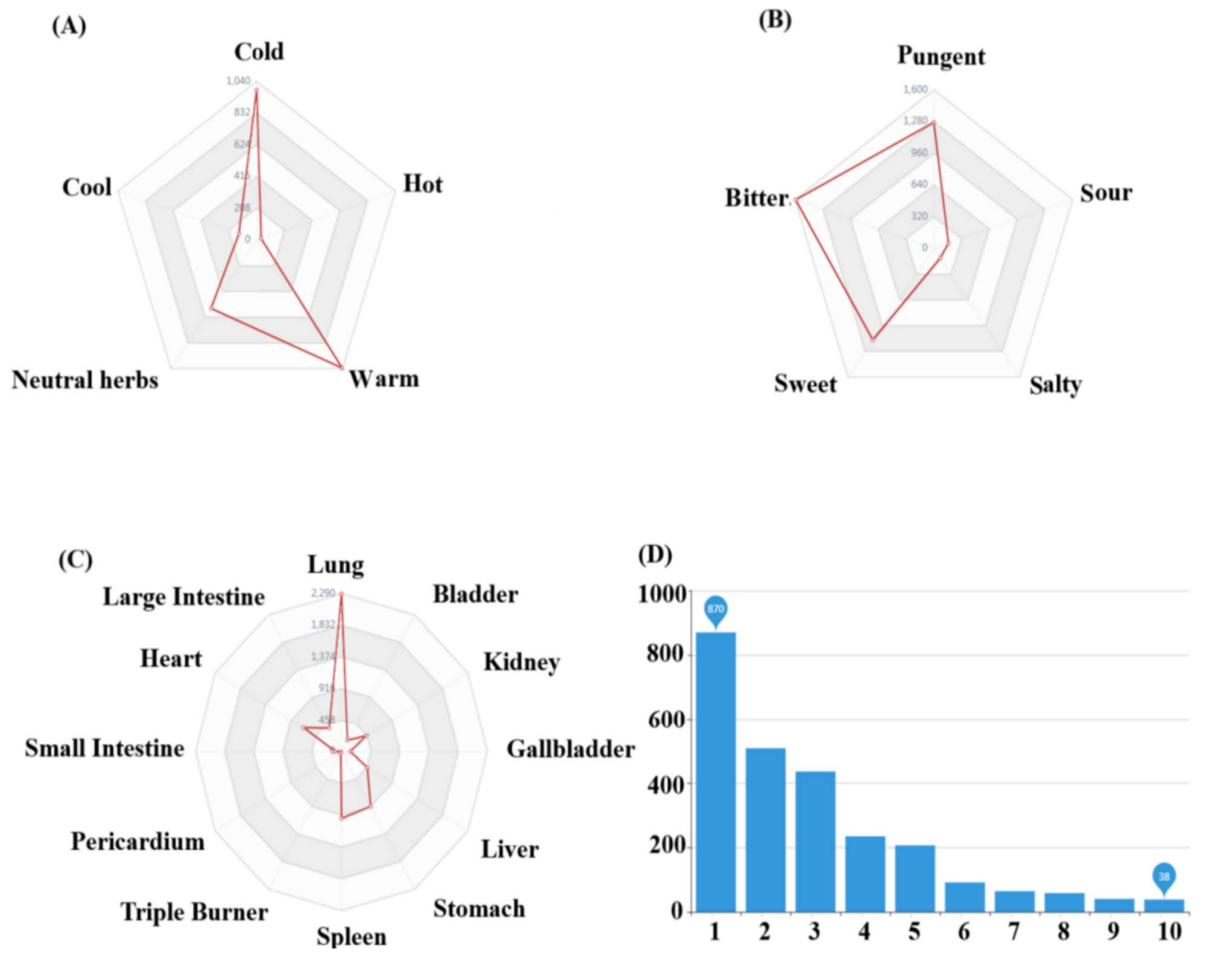

Fig. 2: Analysis of the Four Qi, Five Flavors, Meridian Tropism and Efficacy of Traditional Chinese Medicine in IBV Prescription Data Set. (A) Radar plot showing the statistical analysis of the Four Natures; (B) Radar plot showing the statistical analysis of the Five Tastes; (C) Radar plot showing the statistical analysis of the Meridian Tropism (Gui Jing); (D) Pharmacological Actions statistical chart, where items 1-10 represent: Cough Suppressant, Phlegm-Resolving, and Antiasthmatic; Clearing Heat; Tonifying Deficiency; Releasing the Exterior; Regulating Qi; Astringing (Consolidating) Functions; Promoting Diuresis and Resolving Dampness; Calming the Liver and Extinguishing Wind; Calming the Shen; Digestive Aid.

Herbal frequency profiling: Quantitative analysis of 361 herbs (total occurrence: 2,087) identified 60 high-frequency components (>10 occurrences). The decamerous dominant herbs comprised: Licorice (15.2%), Platycodon (12.8%), Bitter Apricot (11.5%), Fritillaria (9.7%), Ephedra (8.9%), Pinellia (8.3%), Tangerine Peel (7.6%), Perilla (6.9%), Scutellaria (6.2%), and Stemona (5.7%) (Complete ranking in Table 5).

Table 4: Analysis of prescription efficacy

No.	Prescription efficacy	Frequency	Rate
1	Cough Suppressant, Phlegm-Resolving and Antiasthmatic	870	31.78%
2	Clearing Heat	507	18.52%
3	Tonifying Deficiency	435	15.89%
4	Releasing the Exterior	234	8.55%
5	Regulating Qi	206	7.52%
6	Astringing (Consolidating) Functions	91	3.32%
7	Promoting Diuresis and Resolving Dampness	64	2.33%
8	Calming the Liver and Extinguishing Wind	58	2.11%
9	Calming the Shen	40	1.46%
10	Digestive Aid	38	1.39%

Association rule mining: An association rule analysis was performed on the 336 prescriptions and 361 medicinal herbs. The frequency of herb combinations was analyzed with the following parameters: a minimum support of 15% and a confidence of 0.5. Support was set to 56, meaning only herb combinations that appeared 56 times or more in the dataset were included in the results. This analysis identified 14 common herb pairs. For example, the combination of Licorice & Bitter Apricot Kernel appeared 101 times, resulting in support of 10.30%. Support in Table 6 is calculated as the ratio of the number of occurrences of the herb pair to the total number of prescriptions, multiplied by 100%. Confidence refers to the probability that herb B will appear when herb A is present in a prescription. The core associations between herbs were further analyzed and are presented in Table 7 and the topological map of core prescription rules (Fig. 3). For instance, the association rule Platycodon & Bitter Apricot Kernel > Licorice had a confidence of 0.82, meaning that 82% of prescriptions containing Platycodon and Bitter Apricot Kernel also contained Licorice. A confidence threshold of 0.7 was applied, meaning only data with a probability of 70% or higher was considered.

Cluster analysis and formula optimization: Hierarchical clustering (k=5) partitioned prescriptions into five therapeutic clusters in Table 8.

Table 5: Herbal formulations with a prescription frequency greater than 10

No.	Herbal formulations	Frequency	No.	Herbal formulations	Frequency	No.	Herbal formulations	Frequency
1	Licorice (Glycyrrhiza uralensis)	179	21	Anemarrhena (Anemarrhena asphodeloides)	39	41	Asarum (Asarum sieboldii)	17
2	Platycodon (Platycodon grandiflorus)	139	22	Bai Qian (Cynanchum paniculatum)	31	42	Isatis Root (Isatis indigotica)	16
3	Bitter Apricot Kernel (Prunus armeniaca)	135	23	Poppy Shell (Papaver somniferum)	30	43	Radish Seed (Raphanus sativus)	15
4	Fritillaria (Fritillariae cirrhosae Bulbus)	125	24	Trichosanthes (Trichosanthes kirilowii)	28	44	Ginkgo Nut (Ginkgo biloba)	15
5	Ephedra (Ephedra sinica)	114	25	Mustard Seed (Sinapis alba)	27	45	Bletilla (Bletilla striata)	14
6	Pinellia (Pinellia ternata)	100	26	Borneol (Cinnamomum camphora)	27	46	Northern Slippery Root (Codonopsis pilosula var. modesta)	14
7	Tangerine Peel (Citrus reticulata)	98	27	Zhi Ke (Citrus aurantium)	26	47	Cinnabar (Mercury sulfide)	14
8	Perilla (Perilla frutescens)	87	28	Rehmannia (Rehmannia glutinosa)	25	48	Mulberry Leaf (Morus alba)	14
9	Scutellaria (Scutellaria baicalensis)	79	29	Polygala (Polygala tenuifolia)	24	49	Agarwood (Aquilaria sinensis)	13
10	Stemona (Stemona tuberosa)	78	30	Tian Hua Fen (Trichosanthes rosthornii)	22	50	Ginger (Zingiber officinale)	13
11	Mint (Mentha haplocalyx)	72	31	Scrophularia (Scrophularia ningpoensis)	21	51	Pear (Pyrus spp.)	13
12	Mulberry Root Bark (Morus alba)	68	32	Lily (Lilium lancifolium)	19	52	Cattle Gallstone (Bos taurus)	13
13	Gypsum (Gypsum fibrosum)	67	33	Codonopsis (Codonopsis pilosula)	19	53	Donkey-hide Gelatin (Equus asinus)	12
14	Corydalis (Corydalis yanhusuo)	62	34	Asparagus Tuber (Asparagus cochinchinensis)	19	54	Hawthorn (Crataegus pinnatifida)	12
15	Loquat (Eriobotrya japonica)	61	35	Honeysuckle (Lonicera japonica)	18	55	Dried Ginger (Zingiber officinale)	12
16	Ophiopogon (Ophiopogon japonicus)	49	36	Tangerine Peel (Citrus reticulata)	18	56	Zhi Shi (Citrus aurantium)	11
17	Poria (Poria cocos)	48	37	Dried Tangerine Peel (Citrus reticulata)	18	57	Houttuynia (Houttuynia cordata)	11
18	Coltsfoot Flower (Tussilago farfara)	48	38	Cobra Gall (Naja naja)	17	58	Rhubarb (Rheum palmatum)	11
19	Schisandra (Schisandra chinensis)	45	39	Arisaema (Arisaema erubescens)	17	59	Forsythia (Forsythia suspensa)	11
20	Aster (Aster tataricus)	40	40	Gardenia (Gardenia jasminoides)	17	60	White Peony Root (Paeonia lactiflora)	11

Table 6: High frequency combination analysis of prescriptions (15%)

No.	Herb combinations	Rate	Support
1	Licorice, Bitter Apricot Kernel	101	10.30%
2	Licorice, Platycodon	90	9.17%
3	Licorice, Ephedra	82	8.36%
4	Bitter Apricot Kernel, Ephedra	77	7.85%
5	Licorice, Tangerine Peel	74	7.54%
6	Platycodon, Bitter Apricot Kernel	72	7.34%
7	Licorice, Pinellia	67	6.83%
8	Licorice, Bitter Apricot Kernel, Ephedra	63	6.42%
9	Licorice, Fritillaria	62	6.32%
10	Platycodon, Ephedra	60	6.12%
11	Licorice, Platycodon, Bitter Apricot Kernel	59	6.10%
12	Licorice, Perilla	59	6.10%
13	Bitter Apricot Kernel, Perilla	58	5.91%
14	Platycodon, Fritillaria	57	5.81%

Comparison of therapeutic effects in animal experiments

Efficacy rating and daily weight gain: At 3 dpi, the chicks successively exhibited lethargy, reduced appetite, increased water intake, frequent head shaking, droopy wings, coughing, oral breathing, and tracheal rales. Clinical symptoms of IBV-infected chicks were observed and scored at different time intervals (Fig. 4A). During the observation period, both the ribavirin group and the IBV group maintained consistently high symptom scores, whereas the TCM-1 group had the lowest symptom scores after treatment, and the scores of the TCM-2 group were nearly comparable to those of the TCM-5 group. At 14 dpi, the symptom scores of all chicks in the TCM-1, TCM-2 and TCM-5 groups dropped to 0. The IBV group still had over half of the chicks in a diseased status, but its scores were comparable to those of the Ribavirin group, with the condition gradually improving. Throughout the entire observation period, the TCM-1 group exhibited a superior therapeutic effect. The dynamic changes in average daily gain (ADG) of IBV-infected yellow-feathered broilers treated with different TCM preparations were monitored from 0 to 14 dpi (Fig. 4B). At 0 dpi, no significant difference in ADG was observed among all groups. From 1 dpi onward, the ADG growth rate of the IBV model group was markedly slower relative to the NC group. In contrast, all the TCM treatment groups (TCM-1 to TCM-5) showed a more consistent ADG growth trend compared to the NC group; it is notable that the TCM-2 and TCM-3 groups demonstrated a more significant increase in ADG.

Table 7: Analysis of the core associations between herbs rules (confidence 0.5)

No.	Association rules		Confidence level
	A	B	
1	Platycodon, Bitter Apricot Kernel	Licorice	0.82
2	Bitter Apricot Kernel, Ephedra	Licorice	0.82
3	Licorice, Ephedra	Bitter Apricot Kernel	0.77
4	Tangerine Peel	Licorice	0.76
5	Perilla	Licorice	0.76
6	Bitter Apricot Kernel	Licorice	0.75
7	Perilla	Bitter Apricot Kernel	0.74
8	Ephedra	Licorice	0.73
9	Ephedra	Bitter Apricot Kernel	0.68
10	Pinellia	Licorice	0.67
11	Licorice, Platycodon	Bitter Apricot Kernel	0.66
12	Platycodon	Licorice	0.65
13	Licorice, Bitter Apricot Kernel	Ephedra	0.62
14	Licorice, Bitter Apricot Kernel	Platycodon	0.58
15	Licorice	Bitter Apricot Kernel	0.57
16	Bitter Apricot Kernel	Ephedra	0.57
17	Bitter Apricot Kernel	Platycodon	0.53
18	Ephedra	Platycodon	0.53
19	Platycodon	Bitter Apricot Kernel	0.52
20	Licorice	Platycodon	0.51
21	Fritillaria	Licorice	0.5

Table 8: Analysis of medication core combinations

No.	Formula category	Quantity of prescription
1	Licorice, Bitter Apricot Kernel, Platycodon, Perilla, Ephedra, Pinellia	141
2	Licorice, Fritillaria, Tangerine Peel, Bitter Apricot Kernel, Platycodon, Pinellia	93
3	Platycodon, Stemona, Licorice, Bai Qian, Ephedra, Bitter Apricot Kernel	62
4	Scutellaria, Honeysuckle, Licorice, Houttuynia, Ophiopogon, Ephedra	23
5	Rehmannia, Fritillaria, Ophiopogon, Licorice, Borneol, Bitter Apricot Kernel	33

Note: Each formula is the centroid of a cluster from k-means analysis. Herbs are listed in descending order of frequency within the cluster. Equal ratios were used for initial screening.

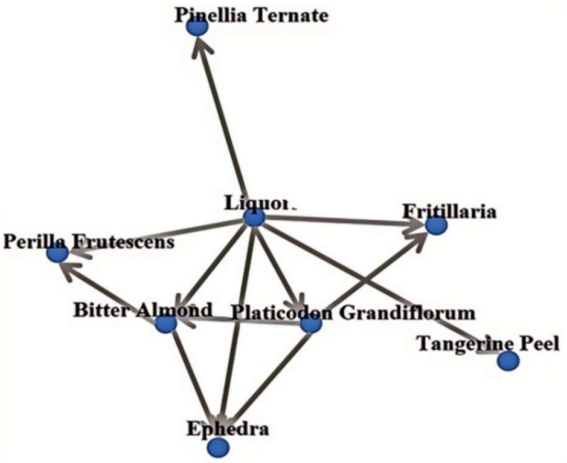

Fig. 3: The topological map of core prescription rules.

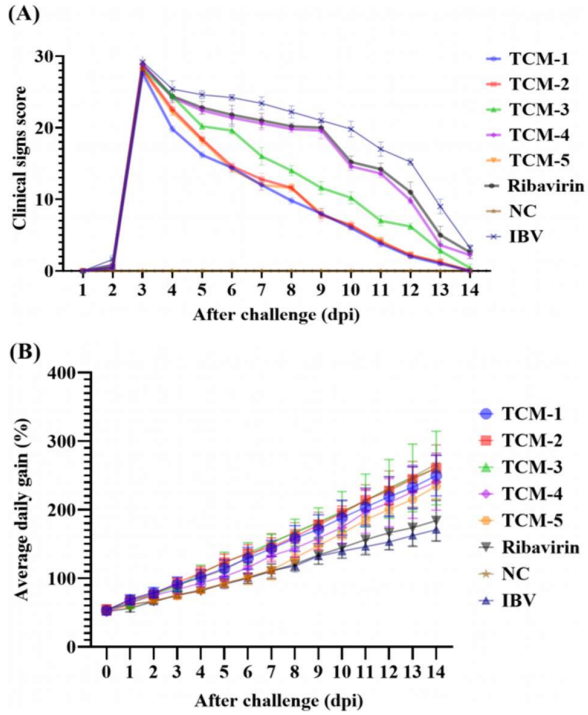

Fig. 4: Clinical signs scores and average daily gain of TCM-treated IBV broilers post-challenge. (A) Temporal changes in clinical signs scores of broilers over 14 days after IBV challenge. (B) Dynamic changes in average daily gain (%) of the groups during 14 dpi.

Effects of TCM preparations on immune organ indices in IBV-infected broilers: The immune organ indices (thymus, spleen, and bursa of Fabricius) of the IBV-infected broilers were measured on the 3, 7, and 14 dpi to evaluate the immune protection mediated by the TCM. In the thymus index (Fig. 5A), the TCM-2, TCM-3, TCM-4, TCM-5, and NC groups showed significantly higher values than the IBV group at 3 dpi ($P<0.05$ to $P<0.001$). At 7 dpi, compared with the IBV group, the TCM-4 group showed a significantly increased thymus index ($P<0.05$). On the 14th day, compared with the IBV group, the TCM-5 group showed a significantly increased thymus index ($P<0.05$). For the spleen index (Fig. 5B), no statistically significant differences were observed between any treatment group and the IBV group at all time points, although the values in some TCM groups increased. Regarding the bursa of Fabricius index (Fig. 5C), the TCM-1, TCM-3, TCM-4, TCM-5, and NC groups showed significantly higher values than the IBV group ($P<0.05$ to $P<0.001$), while the TCM-2 and ribavirin groups did not show any differences. On the 7th day, only the ribavirin group showed a significantly increased index ($P<0.01$). On the 14th dpi, the TCM-2 ($P<0.01$) and TCM-5 ($P<0.05$) groups showed significantly higher indices, while no effects were observed in other groups. In summary, these results indicate that the TCM formulations exerted time- and group-dependent protective effects on the development of the thymus and bursa of Fabricius in IBV-infected broilers, thereby alleviating virus-induced immune suppression, without observing significant regulation of the spleen index.

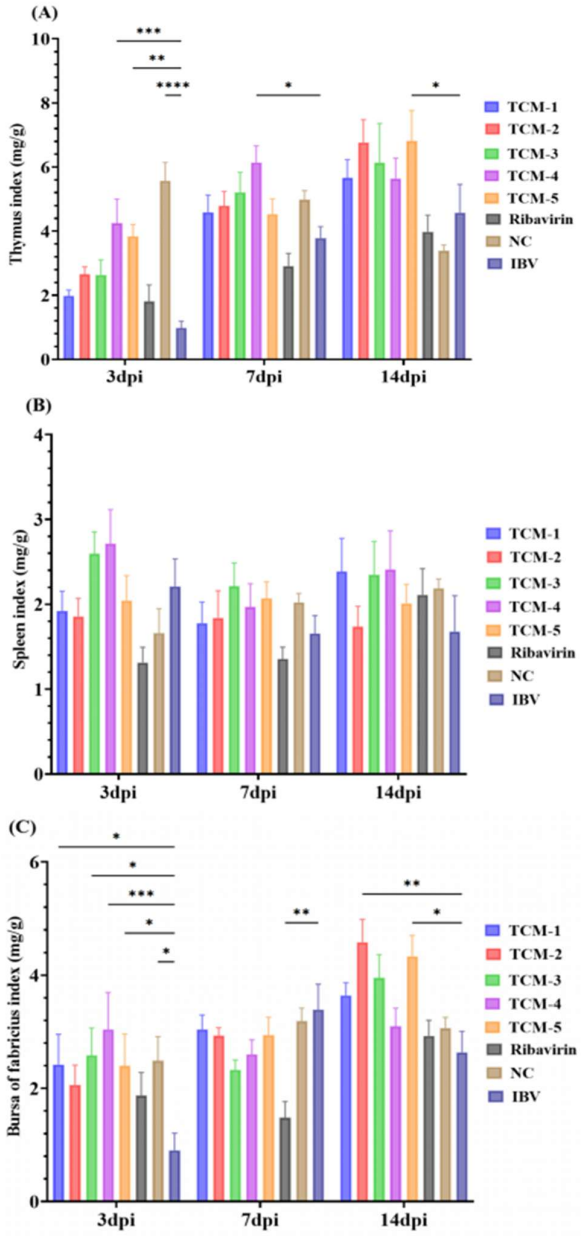

Fig. 5: Immune organ indices of TCM-treated IBV broilers. (A) Thymus, (B) spleen, (C) bursa of Fabricius indices in IBV broilers treated with TCM preparations/ribavirin, detected at 3, 7, 14 dpi. *P<0.05, ***P<0.001, ****P<0.0001 (vs. IBV group).

Effects of TCM preparations on IBV load and antibodies in chicks: To evaluate the antiviral and immunomodulatory effects of TCM preparations, IBV viral loads in trachea and nasal sinus were quantified by qPCR at 3, 7, and 14 dpi, and IBV-specific antibody levels in serum were measured by ELISA. For tracheal viral load at 3 dpi (Fig. 6A), TCM-1, TCM-2, TCM-4, TCM-5, and the NC group exhibited significantly lower viral loads than the IBV group ($P<0.05$ to $P<0.0001$), while TCM-3 and ribavirin groups showed no statistical difference. At 7 dpi (Fig. 6B), only TCM-3 ($P<0.05$) and NC ($P<0.0001$) groups displayed reduced viral loads relative to the IBV group, with no significant effects observed in other TCM preparations or ribavirin; by 14 dpi (Fig. 6B), no significant differences were detected between any treatment group and the IBV group. In nasal sinus, viral loads were significantly decreased in TCM-1, TCM-2, TCM-4, and NC groups at 3 dpi ($P<0.01$ to $P<0.0001$) compared with the IBV group, whereas TCM-3, TCM-5, and ribavirin groups showed no difference (ns). At 7 dpi, TCM-3 ($P<0.05$), TCM-5 ($P<0.01$), and NC ($P<0.0001$) groups exhibited significantly lower viral loads versus the IBV group, with no effects in other groups; by 14 dpi, no significant differences were observed across all treatment groups relative to the IBV group. Regarding IBV-specific antibody response (Fig. 6C), all groups showed near-baseline OD450 values (<0.3) at 3 dpi, with no significant differences. By 7 dpi, partial TCM groups (e.g., TCM-1, TCM-4, TCM-5) displayed a numerical increase in OD450 values, though most remained below the positive threshold of 0.3. At 14 dpi, TCM-2 and TCM-3 groups exhibited significantly elevated OD450 values (>0.3), indicating enhanced antibody production compared with the IBV group. Collectively, these findings demonstrate that TCM preparations exert time- and group-dependent antiviral effects by reducing IBV viral loads in respiratory tissues and promoting specific antibody responses during IBV infection.

Oxidative stress-related indices in TCM-treated IBV-infected chicks: To evaluate the effect of TCM preparations on the oxidative stress response of chicks infected with IBV, the levels of serum nitric oxide (NO), malondialdehyde (MDA), xanthine oxidase (XOD), and total antioxidant capacity (T-AOC) were measured on days 3, 7, and 14. Dunnett's multiple comparison test was used to compare each group with the IBV control group. At 3 dpi (Fig. 7A), compared with the IBV group, the NO concentrations in the TCM-2 ($P<0.0001$), TCM-3 ($P<0.01$), TCM-4 ($P<0.0001$), TCM-5 ($P<0.01$), ribavirin ($P<0.0001$), and NC ($P<0.0001$) groups were significantly increased, while no difference was observed in the TCM-1 group. In the TCM-1 group ($P<0.0001$), TCM-2 ($P<0.0001$), and TCM-3 ($P<0.05$) groups, the T-AOC activity was significantly increased, while no effect was detected in the other groups; compared with the IBV group, there were no statistically significant differences in the MDA and XOD levels of all treatment groups (TCM-1 to TCM-5, $P<0.0001$ to $P<0.05$) and ribavirin ($P<0.05$) and NC ($P<0.0001$). At 7 dpi (Fig. 7B), compared with the IBV group, the NO concentrations in all TCM groups (TCM-1 to TCM-5, $P<0.0001$ to $P<0.05$), ribavirin ($P<0.05$) and NC ($P<0.0001$) were significantly higher, while there were no significant differences in T-AOC, MDA and XOD levels between any treatment group and the IBV group. On the 14th day (Fig. 7C), no statistically significant differences in the levels of NO, T-AOC, MDA, or XOD were observed between any treatment group and the IBV group, although there were numerical trends in some TCM groups. In summary, these findings indicate that TCM preparations have a time-dependent regulatory effect on oxidative stress response, with the most significant effects observed for NO and T-AOC on days 3 and 7, respectively, while there was no sustained effect on MDA or XOD.

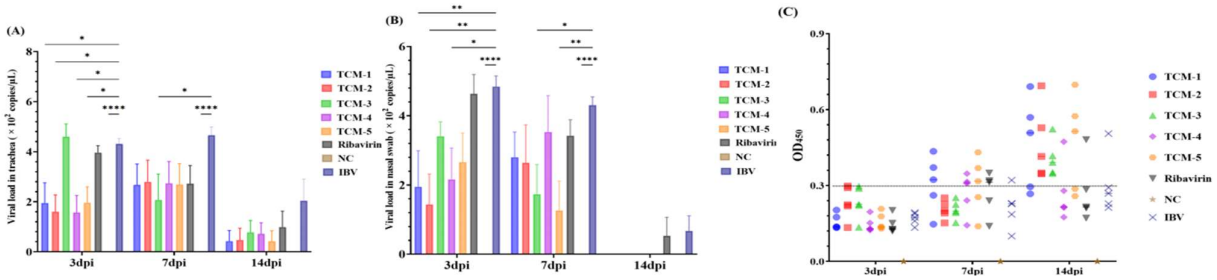

Fig. 6: Tracheal viral load and IBV-specific antibody in TCM-treated IBV chicks. (A-B) Tracheal viral load; (C) Serum IBV-specific antibody levels in TCM/ribavirin-treated IBV chicks at 3, 7, 14 dpi. *P<0.05, ***P<0.001, ****P<0.0001 (vs. IBV group).

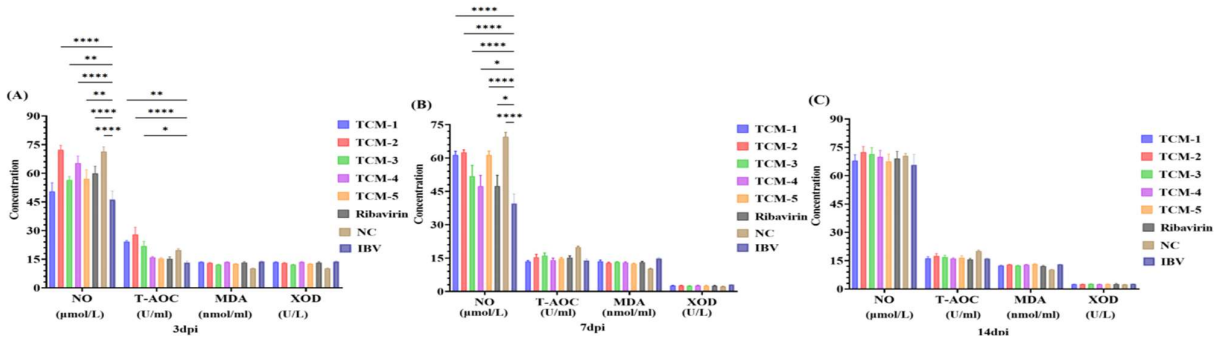

Fig. 7: Serum Oxidative Stress Indices in TCM-Treated IBV Chicks. (A–C) Serum concentrations of NO, T-AOC, MDA, and XOD in IBV-infected chicks treated with TCM preparations or ribavirin, measured at 3, 7, and 14 dpi, respectively. ****P<0.0001, ***P<0.001, **P<0.01, *P<0.05 (vs. IBV group).

Serum inflammatory cytokine levels in TCM-treated IBV chicks: In order to study the immunomodulatory effect of TCM preparations on the inflammatory response of chicks infected with IBV, at 3, 7, and 14 dpi, the concentrations of IL-4, TNF-α, IFN-γ, IL-10, IL-6, and IL-1β in serum were quantitatively determined by ELISA, and the differences were evaluated using Dunnett's multiple comparison test. At 3 dpi (Fig. 8A), the IL-4 levels in the TCM-3 ($P<0.01$), TCM-5 ($P<0.05$), and NC ($P<0.001$) groups were significantly increased, while only the TNF-α level in the NC group was significantly increased ($P<0.05$); there were no significant differences in the levels of IFN-γ, IL-10, and IL-6 among all treatment groups. It is notable that compared with the IBV group, the IL-1β concentrations in all TCM groups, the ribavirin group, and the NC group were significantly higher ($P<0.0001$). At 7 dpi (Fig. 8B), IL-4 levels were significantly increased in TCM-2 ($P<0.01$), TCM-3 ($P<0.01$), TCM-4 ($P<0.05$), TCM-5 ($P<0.01$) and NC ($P<0.0001$) groups, and TNF-α levels were elevated in TCM-1 ($P<0.05$), TCM-2 ($P<0.01$), TCM-3 ($P<0.01$), TCM-4 ($P<0.01$), TCM-5 ($P<0.01$), and ribavirin ($P<0.01$) groups. The levels of IFN-γ in the TCM-1 ($P<0.05$), TCM-2 ($P<0.05$), TCM-3 ($P<0.05$), TCM-5 ($P<0.05$) and NC ($P<0.01$) groups were significantly higher. The levels of IL-10 in all TCM groups, ribavirin and NC ($P<0.01$) groups were also higher. There was no significant difference in IL-6 levels among the Chinese medicine 2 group ($P<0.0001$), Chinese medicine 3 group ($P<0.0001$), Chinese medicine 5 group ($P<0.001$) and the control group ($P<0.0001$), while the IL-1β levels were significantly increased. At 14 dpi (Fig. 8C), IL-4 levels were significantly higher in TCM-1 ($P<0.05$), TCM-2 ($P<0.05$), TCM-3 ($P<0.05$), TCM-5 ($P<0.05$) and NC ($P<0.01$) groups, while TNF-α, IFN-γ, IL-10, and IL-6 levels showed no significant differences across all treatment groups (ns). IL-1β concentrations remained significantly elevated in TCM-1 ($P<0.0001$), TCM-2 ($P<0.01$), TCM-3 ($P<0.0001$), TCM-4 ($P<0.01$), ribavirin ($P<0.0001$) and NC ($P<0.0001$) groups. In conclusion, these findings indicate that the TCM preparations exert a time-dependent and cytokine-dependent regulatory effect on inflammatory responses. On the 7th day, the most significant effects were observed on IL-4, TNF-α, IFN-γ, IL-10, and IL-1β, suggesting a potential role in regulating the pro-inflammatory and anti-inflammatory cytokine networks during IBV infection.

SEM analysis of tracheal villus damage in TCM-treated IBV chicks: SEM was used to evaluate the ultrastructural morphology of the tracheal cilia of chicks at 7 dpi (Fig. 9). The control group showed dense and regularly arranged tracheal cilia, with a completely intact and well-organized surface morphology. In contrast, the IBV model group exhibited extensive loss of tracheal cilia, almost completely depleted, accompanied by obvious surface swelling and protrusion. This group showed severe structural damage consistent with the pathological injury induced by IBV. In the treatment groups, the Chinese medicine 4 group and the Chinese medicine 5 group retained some tracheal cilia, with relatively regular arrangement, and minor cilia loss. Compared with the IBV group, their structural damage, including no obvious surface swelling, was significantly reduced. Compared with the IBV group, the TCM-1, TCM-2 and TCM-3 groups showed reduced cilia loss, but a significant portion of the cilia was still missing, with slight structural disorder. Compared with the IBV group, the ribavirin group showed reduced cilia loss, but its cilia consumption was more severe than the TCM-4 and TCM-5 groups, with slight residual irregularity in the structure. In summary, TCM-4 and TCM-5 provided the best protection of tracheal ciliary integrity, whereas TCM-1, TCM-2, and TCM-3 showed moderate effects, and ribavirin was less effective than TCM-4/5.

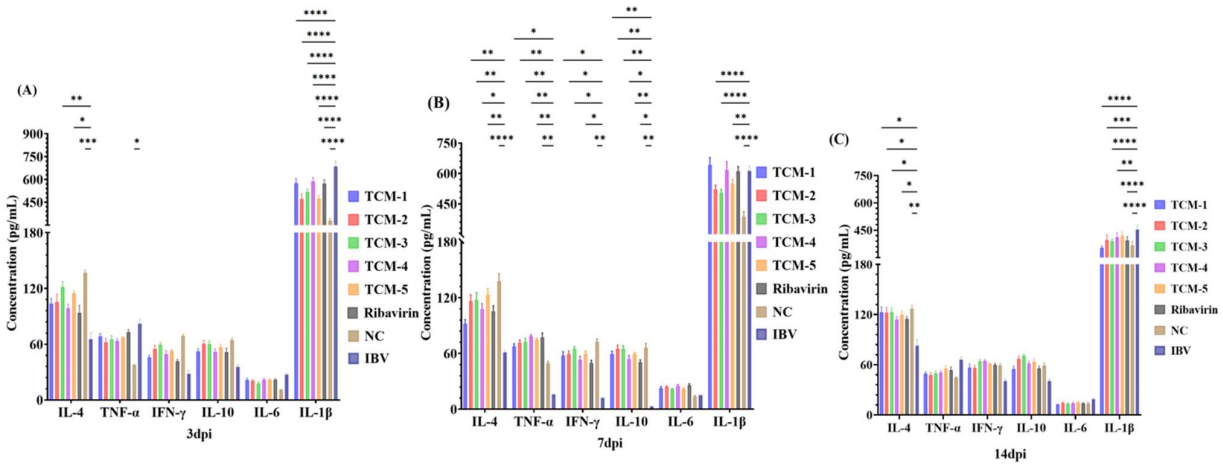

Fig. 8: Serum Inflammatory Cytokines in TCM-Treated IBV Chicks. (A–C) Serum concentrations of IL-4, TNF-α, IFN-γ, IL-10, IL-6, IL-1β in IBV-infected chicks treated with TCM preparations or ribavirin, measured at 3, 7, and 14 dpi, respectively. *P<0.05, **P<0.01, ****P<0.0001 (vs. IBV group).

Histopathological observation of lung tissue in TCM-treated IBV chicks: Histopathological changes of lung tissues were observed in chicks at 7 dpi (Fig. 10). The NC group showed intact lung tissue structure. The morphology of primary bronchi, parabronchi and respiratory capillaries was normal, and no pathological changes (including hemorrhage, congestion, edema or cell necrosis) were identified. In contrast, the IBV model group exhibited obvious pathological damage in lung tissues. Parabronchial structure was unclear, with a small amount of necrotic cell debris present. Occasional hemorrhage in parabronchi, capillary/interstitial vascular congestion and perivascular edema in interstitium were also observed, accompanied by loose connective tissue (corresponding to black, yellow and orange arrows, respectively). TCM-1, TCM-2 and TCM-5 groups showed mild pathological damage. Only occasional slight interstitial vascular congestion was noted, with no obvious hemorrhage, edema or necrotic debris. TCM-3 group presented a small amount of parabronchial congestion and interstitial edema, but no necrotic cell debris. TCM-4 group had only occasional minor hemorrhage in parabronchi, while other structures remained relatively intact. The Ribavirin group showed a small number of goblet cells in primary bronchi, small amounts of eosinophilic substances in the lumen, and mild thickening of respiratory capillary walls in small areas (corresponding to green and blue arrows, respectively). The degree of pathological damage in this group was significantly lighter than that of the IBV group. In summary, all TCM formulations alleviated IBV-induced lung pathology to varying degrees, with TCM-1, TCM-2, TCM-5, and ribavirin showing the mildest lesions, while TCM-3 and TCM-4 exhibited intermediate protection.

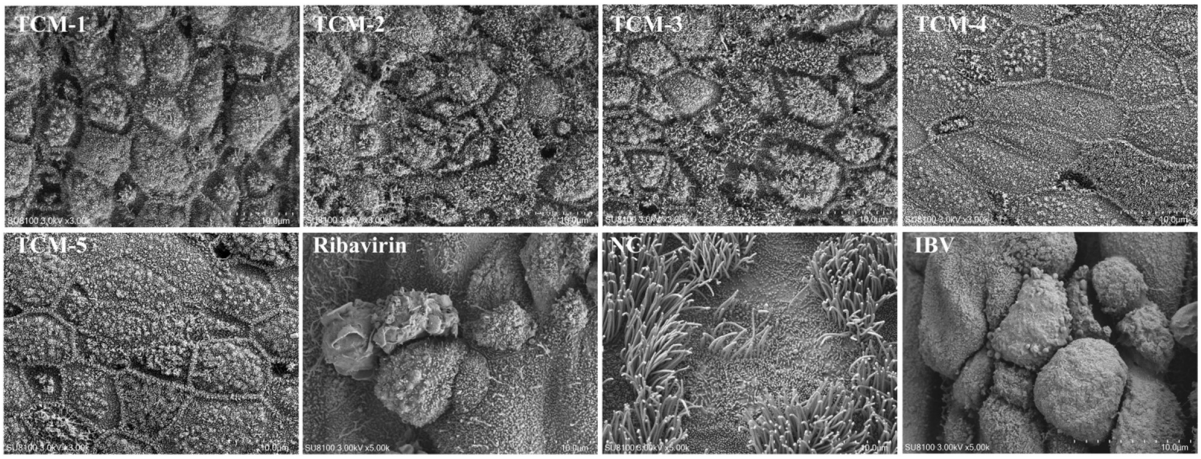

Fig. 9: Tracheal Ciliary Ultrastructure of TCM-Treated IBV Chicks via SEM. Scale bar: 10.0 Mm.

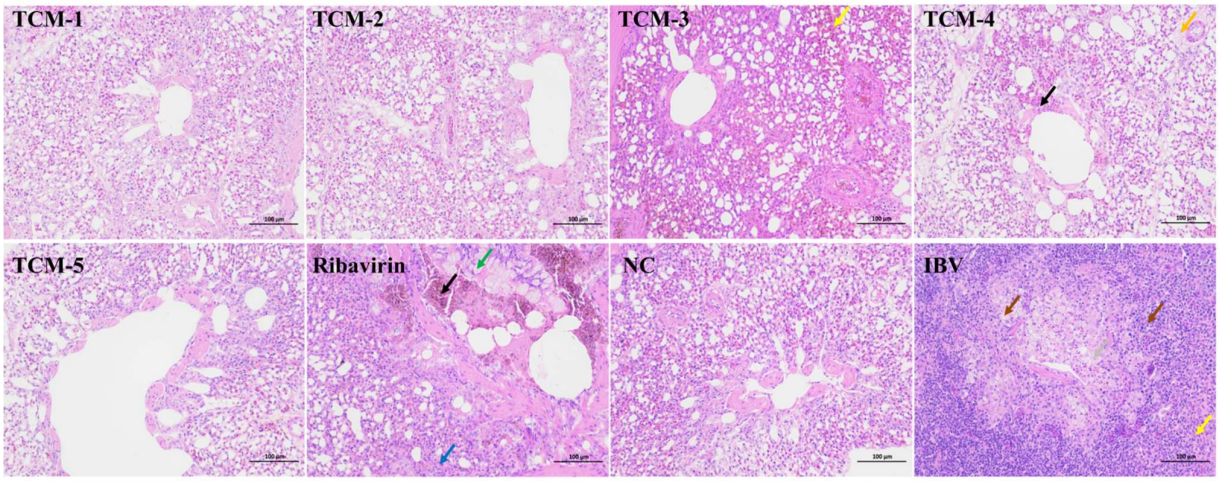

Fig. 10: Lung Histopathological Changes in TCM-Treated IBV Chicks at 7 dpi. Arrows indicate: black = parabronchial hemorrhage; yellow = vascular congestion; orange = perivascular edema; green = goblet cells; blue = respiratory capillary wall thickening. NC displays intact structure; IBV shows severe pathological lesions.

DISCUSSION

IBV is the main pathogenic virus threatening the global poultry industry. It is highly contagious and can cause severe respiratory diseases and systemic disorders in chickens, resulting in increased mortality rates among chickens, reduced egg production in egg-laying hens, and significant economic losses (Rafique *et al*., 2024). The current IBV prevention and control strategies mainly rely on vaccine immunization and chemical antiviral agents

(Liu *et al*., 2024). However, IBV exhibits a high degree of genetic variation and many serotypes, resulting in insufficient cross-protection provided by traditional vaccines (Zhang *et al*., 2021). The long-term use of chemical drugs often leads to the development of drug resistance in viruses, and the presence of drug residues poses a risk to public health, highlighting the serious limitations of the existing control measures (Zhao *et al*., 2023). TCM has emerged as a promising alternative for managing livestock and poultry viral diseases, owing to its unique advantages including multi-target regulation, low toxicity, and minimal residues (Sun *et al*., 2014; Yurdakok-Dikmen *et al*., 2018; Zhang *et al*., 2020). However, the development of anti-IBV TCM formulas has long been constrained by empirical methods, lacking systematic big data support and modern technological guidance, which has hindered the realization of precise targeted drug development. Therefore, overcoming the bottlenecks of TCM empirical research, establishing a TCM formula research and development system based on modern big data technology, and integrating the "diagnosis and treatment based on syndrome differentiation" theory of TCM with the needs of precise prevention and control, has become a scientific issue that urgently needs to be addressed in the modernization of TCM and the green management of IBV (Li, 2016).

This study innovatively adopted a cross-disciplinary approach to apply the TCM Inheritance Computing Platform V3.0 (hereafter referred to as the Platform) to anti-IBV TCM formula development, establishing a standardized research workflow involving TCM big data mining, core formula clustering and animal experiment verification (Wang *et al*., 2018). First, the Platform was utilized to integrate 34,324 marketed traditional TCM prescriptions, 7,505 TCM patent medicines, and 4,207 formulas from the TCM Inheritance Database, screening out 336 candidate formulas that matched the clinical phenotypes of IBV infection. Subsequently, association rules and cluster analysis were conducted to clarify the compatibility rules of the core drug pairs and identify five types of core prescriptions with different therapeutic effects. Finally, through animal experiments, the therapeutic effects of five TCM preparations on IBV-infected white-feathered broiler chickens were systematically evaluated. The comprehensive anti-IBV mechanisms of these preparations were elaborated from multiple dimensions such as alleviation of clinical symptoms, recovery of growth performance, regulation of immune function, virus clearance, regulation of oxidative stress, inhibition of inflammatory response, and improvement of histopathology. This provided a solid experimental basis for the clinical application of TCM in IBV control and further research on potential target points for its potential effects.

TCM has a history of over 4,000 years. Its empirical knowledge and systematic documentation have evolved into a complex treatment system for various diseases (Ma *et al*., 2025). The Platform is an auxiliary system for TCM inheritance and research and development (R&D), constructed based on big data mining and intelligent analysis technologies, which provides robust technical support for the preservation of TCM theories and the optimization of clinical diagnosis and treatment (He *et al*., 2012; Zuo *et al*., 2015; Ren *et al*., 2023). Initially designed for mining and optimizing human TCM formulas, the Platform has been successfully applied to analyze staging syndrome differentiation and acupoint selection rules for peripheral facial paralysis (Wang, 2023); establish a TCM prescription database for palpitations and explore its medication rules (Dai *et al*., 2018); analyze the regularity of umbilical application of TCM in the treatment of cirrhotic ascites (Sun *et al*., 2017); analyze and summarize the composition principles of traditional TCM prescriptions for nausea (Han *et al*., 2016); investigate the prescription regularity of diarrhea in clinical practice guidelines for traditional Chinese medical practitioners to discover new TCM agents for diarrhea treatment (He & Zhu, 2016); and explore the composition and medication rules of prescriptions for angina pectoris to develop new TCM agents for angina pectoris therapy (Zhao & Teng, 2015). Building on this experience in summarizing TCM medication rules, this study drew an analogy between the pathological features of IBV-infected chickens (e.g., respiratory mucosal damage and immune dysfunction) and the human TCM syndrome of "failure of lung qi to disperse and descend, phlegm-heat stagnating in the lung" (Zhou-Suckow *et al*., 2017; Ganapathy, 2021; Su & Xiong, 2021; Mikami *et al*., 2023). This analogy provides a critical theoretical foundation for translating human TCM big data to TCM R&D, effectively avoiding targeting deviations caused by unguided data migration. The core formulas screened by the Platform exhibited distinct targeting characteristics in terms of four natures and five flavors, meridian tropism, and therapeutic efficacy: warm and cold herbs accounted for similar proportions; sweet, acrid, and bitter flavors dominated; herbs tropic to the lung, spleen and stomach meridians were the most frequently used; and their core efficacies focused on relieving cough, resolving phlegm, alleviating asthma, clearing heat, and tonifying deficiency - all of which are highly consistent with the respiratory symptoms induced by IBV infection (Feng *et al*., 2024).

Association rule and clustering analyses further revealed the core compatibility rules of anti-IBV TCM formulas. The highest confidence levels were observed for the herb pairs Platycodon grandiflorum + Armeniaca vulgaris var. ansu to Liquorice and Armeniaca vulgaris var. ansu + Ephedra sinica to Glycyrrhiza uralensis. Liquorice also occupied a central position in the association rule network topology, as it can restore systemic homeostasis and act as a "guiding herb" to harmonize the effects of other components in TCM prescriptions (Prajapati *et al*., 2026). Additionally, liquorice is rich in bioactive constituents, primarily triterpenoids, flavonoids, and polysaccharides (Wu *et al*., 2025). Modern pharmacological studies have demonstrated its diverse biological activities, including anti-inflammatory, analgesic, anti-cancer, antiviral, antioxidant, and hepatoprotective effects (Zhang *et al*., 2021; Wang *et al*., 2025). Most of the key herbs identified in the association rule network have been reported to possess antiviral activity against coronaviruses (Schlittenlacher *et al*., 2022). For instance, Perilla frutescens leaf extract inhibits SARS-CoV-2 through direct viral inactivation (Tang *et al*., 2021; Chin *et al*., 2022; Dissook *et al*., 2022). Systematic reviews and meta-analyses have identified Liquorice, *Pinellia ternata* and

Bitter almond as the most frequently used Chinese herbs for alleviating COVID-19 clinical symptoms (Xiong *et al*., 2020). Electronic medical record data from hospitals in Wuhan, China, demonstrated that Citrus reticulata peel, *Scutellaria baicalensis* and *Pinellia ternata* ameliorate COVID-19 symptoms by clearing heat and resolving phlegm (Shu *et al*., 2020). Clinical data mining further revealed that the Glycyrrhiza uralensis-*Pinellia ternata* herb pair is a potential candidate against moderate COVID-19, exerting its effects via dual binding to the IL-6/STAT3 signaling pathway (Luo *et al*., 2022). The main active components of *Fritillaria cirrhosa* have also been reported to directly inhibit the cellular entry of SARS-CoV-2 variants by blocking the interaction between the viral spike protein and angiotensin-converting enzyme 2 (ACE2) (Ma *et al*., 2020; Wang *et al*., 2022). Network pharmacology, molecular docking, and experimental studies have validated the therapeutic efficacy of the Bitter almond + Liquorice herb pair against COVID-19 (Yang *et al*., 2020; Hong *et al*., 2023). *Platycodon grandiflorum* acts as a potential broad-spectrum antiviral agent with antiviral and immunomodulatory properties in viral diseases (Gao *et al*., 2025); notably, its major active components can function as inhibitors of SARS-CoV-2 entry (Gurung *et al*., 2022). Bioactive compounds derived from the Ephedra sinica + Liquorice herb pair exhibit strong binding affinity to COVID-19-related targets (Li *et al*., 2021). Specifically, the extract of ephedra binds to ACE2 with high affinity, acting as a blocker to prevent the virus from attaching (Sadeghi*et al*., 2023). Furthermore, the citrus peel extract reduces the replication of the novel coronavirus by regulating the Rho GTPase, PI3K-AKT and MAPK/ERK signaling pathways, and inhibits the formation of syncytia mediated by the spike protein of the novel coronavirus (Bostancikliogl*u et al*., 2024; Kumara *et al*., 2025). IBV and SARS-CoV belong to the same virus family and share similarities in terms of genomics and pathogenesis (Quinteros *et al*., 2022). The infectious bronchitis coronavirus pneumonia model provides new insights into the transmission route of the novel coronavirus (Nefedova *et al*., 2021). Therefore, based on the reported mechanisms of these herbs in combating the novel coronavirus, we can identify the potential antiviral mechanisms of the five formulations in the associated rule network topology of this study, and preliminarily clarify the antiviral effects of these five formulations against the IBV virus.

After infection, IBV mainly targets the epithelial cells of the chicken respiratory tract, causing damage to the airway mucosa, shedding of cilia, and inflammatory responses, manifesting as depression, coughing and respiratory rales (Liu *et al*., 2024). At the same time, it induces immune stress and digestive dysfunction, resulting in slow growth of broiler chickens (Suhail *et al*., 2025). The results showed that chickens infected with IBV exhibited persistent respiratory symptoms, and ribavirin had limited effect in alleviating these symptoms. In contrast, the TCM preparations, especially TCM-1, maintained a lower symptom score throughout the experiment and completely relieved the symptoms at 14 dpi. TCM-2 and TCM-5 also achieved complete symptom relief at this time point. This indicates that the TCM preparations alleviate respiratory damage caused by IBV by inhibiting virus replication, reducing mucosal inflammation, and promoting ciliary repair. In terms of growth performance, the IBV model group had significantly lower ADG than the normal control group, while all the Chinese medicine groups showed a trend closer to the control group's ADG, with significant weight gain advantages for TCM-2 and TCM-3. This finding substantiates the existence of inter-group differences in the regulatory effects of different TCM preparations against IBV infection, and such variations in therapeutic efficacy may be attributed to the multi-pharmacological properties of TCM herbs. On the one hand, they alleviate respiratory tract damage by inhibiting viral replication, thus rapidly relieving clinical symptoms (Chen *et al*., 2020); on the other hand, they enhance nutrient absorption through modulating host metabolic and immune functions, thereby reversing the growth retardation induced by viral infection (Chen *et al*., 2022).

The thymus, spleen, and bursa of Fabricius are core chicken immune organs governing T cell maturation, immune regulation, and B cell differentiation, respectively (Zhang *et al*., 2020; Tian *et al*., 2023). IBV infection induces immune organ atrophy and immunosuppression via apoptosis and inflammatory infiltration (Najimudeen *et al*., 2020; Sun *et al*., 2021; Najimudeen *et al*., 2023). This study found TCM preparations exerted time- and group-dependent protective effects on the thymus and bursa of Fabricius but not the spleen. At 3 dpi, TCM-2, TCM-3, TCM-4, and TCM-5 all increased the thymus index, inhibited early thymocyte apoptosis, and maintained the T cell maturation microenvironment. Only TCM-4 maintained this advantage at 7 dpi, while TCM-5 performed best at 14 dpi, reflecting the time window differences related to the pharmacokinetics and targeting pathways of the active ingredients. For the bursa of Fabricius, TCM-1, TCM-3, TCM-4, and TCM-5 all showed an increase in index at 3 dpi, ribavirin only worked at 7 dpi, and TCM-2 and TCM-5 regained the advantage at 14 dpi. This indicates that the TCM formulation provides continuous protection during the early infection and recovery stages by promoting B cell proliferation and humoral immune homeostasis, while the effect of ribavirin is limited to the middle stage. No significant difference in spleen index was observed between the two groups, which may be due to the tolerance of the spleen to IBV damage, highlighting the time and targeting differences mediated by TCM in immunological protection (Jiang *et al*., 2022). Ribavirin demonstrated a weaker ability to induce antibodies compared to the TCM preparations, highlighting the latter's advantage in activating the adaptive immune system (Wen *et al*., 2024).

IBV invades the host through cilia adhesion, replicates in the trachea and lung tissues and causes damage to the mucosal barrier and viral transmission. The tissue damage is correlated with the viral RNA load (Cavanagh, 2007; Okino *et al*., 2017; Yang *et al*., 2018; Sultan *et al*., 2019). Unlike ribavirin, TCM-1, TCM-2, TCM-4, and TCM-5 inhibited early viral replication in epithelial cells through active components such as polysaccharides and flavonoids at 3 dpi or significantly reduced the viral load in the trachea by enhancing innate

mucosal immunity. Only TCM-3 maintained significant viral inhibition at 7 dpi, indicating that some preparations focus on early blocking, while TCM-3 exhibits a sustained mid-term effect, which may be due to different metabolic rates of active components and targeting replication stages. Nasal sinus viral load detection confirmed the differences in tissue targeting: TCM-1, TCM-2, and TCM-4 inhibited nasal sinus replication at 3 dpi, while TCM-3 and TCM-5 were dominant at 7 dpi. Regarding the antibody response, the level was at the baseline at 3 dpi, showed an increase in some TCM groups at 7 dpi, and significantly exceeded the positive threshold of TCM-2 and TCM-3 at 14 dpi. This delayed immune enhancement supplements the viral load dynamics, with early direct antiviral effects and late antibody-mediated protective effects. Scanning electron microscopy results showed that TCM-4 and TCM-5 maintained the integrity of tracheal cilia, maintained the mucosal barrier function, alleviated respiratory symptoms, and lung tissue pathology confirmed that the TCM preparations were more effective in relieving congestion, edema, bleeding, and necrosis than ribavirin. It suggests that the TCM preparations can protect the integrity of tracheal cilia and maintain the function of the respiratory mucosal barrier (Tamaoki *et al*., 1996; Zhou *et al*., 2022). The mechanical clearance function of cilia is the first line of defense against the invasion of IBV (Becker *et al*., 2024). The protective effect of TCM preparations on cilia can not only reduce IBV adsorption and invasion, but also facilitate the excretion of respiratory secretions, thereby alleviating symptoms such as cough and respiratory rales (Campos-Gomez *et al*., 2023). Lung histopathological findings further confirmed that TCM preparations can alleviate IBV-induced pulmonary congestion, edema, hemorrhage, and necrosis, with efficacy significantly superior to that of the ribavirin-treated group.

IBV infection induces excessive ROS production, triggering oxidative stress characterized by NO overproduction, reduced T-AOC, and accumulation of MDA and XOD (Zhang *et al*., 2022; Han *et al*., 2024). Excessive NO can induce respiratory epithelial cell damage (Moratin *et al*., 2025). As a lipid peroxidation product reflecting cellular oxidative damage levels, MDA and T-AOC, a key metric for evaluating the host's antioxidant capacity, are combined to determine the extent of cellular oxidative stress (Ekin *et al*., 2021). XOD activation represents a key pathway for ROS generation (Wu *et al*., 2023). At a resolution of 3 dpi, the NO concentrations in TCM-2, TCM-3, TCM-4, and TCM-5 significantly increased, while TCM-1, TCM-2, and TCM-3 also showed an increase in T-AOC, without significant accumulation of MDA or XOD. This indicates that the increase in NO induced by the TCM is an immune regulatory signal, rather than a by-product of oxidative damage, and the enhanced antioxidant capacity controls ROS-mediated lipid peroxidation. On the 7th day, NO remained elevated in all TCM groups, while T-AOC, MDA, or XOD did not show significant differences, meaning that NO is involved in inflammatory signal transduction. By the 14th day, all oxidative stress indicators returned to the levels of the IBV group, confirming that the TCM mainly regulates oxidative stress in the early and middle stages, without persistent damage.

Oxidative stress is closely related to inflammatory responses because excessive ROS activates NF-κB and other pathways, inducing the release of pro-inflammatory cytokines (TNF-α, IL-6, IL-1β) and inhibiting anti-inflammatory cytokines (IL-4, IL-10), thereby triggering an inflammatory storm (Sun *et al*., 2024; Wang *et al*., 2025). The regulation of inflammatory cytokines by TCM preparations is time-dependent and cytokine-dependent. On the third day, IL-1β levels increased in all the TCM groups, ribavirin, and the normal control group, while IL-4 only increased in the TCM-3 and TCM-5 groups. This indicates an early innate immune activation through IL-1β and partial anti-inflammatory regulation by IL-4. At 7 dpi, pro-inflammatory and anti-inflammatory cytokines in all groups significantly increased, reflecting an active inflammatory stage. During this stage, TCM balanced antiviral immunity and tissue protection by synchronously regulating the cytokine network, thereby maintaining homeostasis in the body. On the 14th day, only IL-4 and IL-1β remained elevated, indicating the later resolution of inflammation and promotion of immune repair. Ribavirin showed weaker cytokine regulation than TCM-2 and TCM-4, highlighting the advantages of TCM over single-component chemical drugs in terms of immune pathway regulation and interference with the IBV life cycle, being multi-component and multi-targeted (Zheng *et al*., 2025). Overall, TCM preparations can inhibit excessive inflammatory responses by balancing the inflammatory cytokine network (Tie *et al*., 2025). This regulatory effect not only reduces the inflammatory infiltration in lung tissues and respiratory tracts but also prevents the damage to immune organs caused by inflammatory cytokines, thereby creating favorable conditions for the recovery of immune function (Yu *et al*., 2024).

This experiment integrates the results of clinical symptoms, immune organ function, viral load, and the oxidative stress-inflammation response axis. The anti-IBV effect of the TCM formulation is achieved through phased and multi-step synergistic regulation rather than a single target action. For example, TCM-1 optimizes growth recovery, TCM-3 shows excellent mid-term virus clearance rate, although the early response is delayed. TCM-2 and TCM-3 perform well in immune activation, most formulations outperform ribavirin in oxidative stress and inflammation regulation, TCM-5 protects the tracheal cilia and effectively alleviates symptoms, and TCM-4 shows the weakest overall efficacy. The efficacy of the TCM formulations is manifested in three stages. In the early stage (3 dpi), the focus is on inhibiting IBV replication in the trachea and sinuses, enhancing antioxidant capacity, regulating NO release, reducing oxidative damage, and protecting immune organs. In the mid-stage (7 dpi), the focus shifts to immune organ repair and inflammation balance through thymus and Bursa of Fabricius regulation, and some formulations maintain virus suppression. In the later stage (14 dpi), priority is given to specific antibody induction and immune repair consolidation to achieve complete symptom resolution and growth recovery. These differences arise from the different active component compositions and ratios targeted at different virus replication stages and immune pathways. Specific components and targets need to be further clarified through component analysis and in vitro

experiments to guide the best formulation screening and formula optimization (Houeze *et al*., 2023).

This study's value lies in its innovative use of the Platform to construct an anti-IBV drug database and screen 5 effective formulas via data mining, verified by animal experiments. This screening model can be extended to other livestock and poultry diseases, shortening drug discovery and reducing *in-vivo* testing needs. Dynamically tracking key indicators throughout infection clarified stage-specific roles of TCM preparations, providing a more accurate reflection of regulatory processes than traditional single-indicator, single-time-point studies. Compared with ribavirin's weak middle-stage bursa protection and lack of obvious antiviral/immunomodulatory effects, TCM preparations offer comprehensive protection that meets clinical needs and aligns with green poultry farming trends of reducing chemical drug use (Lillehoj *et al*., 2018).

Nevertheless, this study has limitations. The core bioactive components of TCM preparations have not yet been determined, which hinders the clarification of the "component-target-effect" relationship. The regulatory effects on oxidative stress and inflammation are only explored at the overall level, without in-depth analysis of the activation of downstream signaling pathways. The five core formulas were derived from clustering analysis using equal herb ratios. While this approach is suitable for initial screening, it does not reflect optimal clinical compatibility or potential synergistic interactions. The equal-ratio design may underestimate or overestimate the efficacy of certain formulas. The choice of k=5 was based on statistical and interpretability criteria; other clustering solutions might yield different groupings. Therefore, the five formulas should be viewed as representative candidates rather than definitive. The sample size per time point (n=5) is relatively modest. Therefore, the results should be interpreted as preliminary. Future studies with larger sample sizes and across multiple independent cohorts would help to confirm and extend these findings. Animal experiments use a single IBV strain, and the efficacy of different serotypes needs to be verified. Future research should adopt high-performance liquid chromatography (HPLC) to identify the core components, clarify the direct inhibitory effect and targets through in vitro cell experiments, and use transcriptomics and proteomics to elucidate the molecular mechanisms of immune regulation, oxidative stress inhibition, and inflammation regulation (Li *et al*., 2024; Wang *et al*., 2026). The formulation with the best overall efficacy should undergo multi-strain challenge tests and field trials to verify its clinical applicability and safety, providing data support for industrialization.

Declaration of competing interest: We declare that we have no financial and personal relationships with other people or organizations that can inappropriately influence our work, and there is no professional or other personal interest of any nature or kind in any product, service and/or company that could be construed as influencing the content of this paper.

Authors contribution: HL: Conceptualization, validation, Writing – original draft; XW: Data curation, Formal analysis; SP: Investigation, Visualization; CW: Formal analysis, Methodology; MAM: Visualization; YSM: Software; FS: Validation; HS: Project administration; LY: Supervision; BX: Funding acquisition, Writing – review & editing.

Acknowledgements: We warmly thank the Guangxi University professor MeiLan Mo Shared IBV M41 strains. The animal experiments were approved by the Animal Protection and Welfare Committee of Guangxi University (approval number GXU-2021-105) and were conducted in accordance with the ethical guidelines and approved protocols. The authors extend their appreciation to the Princess Nourah bint Abdulrahman University Researchers Supporting Project number (PNURSP2026R224), Princess Nourah bint Abdulrahman University, Riyadh, Saudi Arabia. The authors also acknowledge the Large Research Project funded by the Deanship of Research and Graduate Studies at King Khalid University (R.G.P.2/268/46).

Funding: This work was jointly supported by the Yunnan Province International Science and Technology Commissioner Recognition Work Project (Grant No. 202403AK140025), Young Talent Project of the "Xing Dian Talent Support Program" of Yunnan Province (Grant No. XDYC-QNRC-2023-0424), the Princess Nourah bint Abdulrahman University Researchers Supporting Project number (PNURSP2026R224), Princess Nourah bint Abdulrahman University, Riyadh, Saudi Arabia and the Large Research Project funded by the Deanship of Research and Graduate Studies at King Khalid University (R.G.P.2/268/46).

Appendix supplementary data: The datasets supporting the conclusions of this article are included within the article (and its Additional file).

REFERENCES

Abbas G, Yu J, Li G, 2022. Novel and alternative therapeutic strategies for controlling avian viral infectious diseases: focus on infectious bronchitis and avian influenza. Frontiers of Veterinary Science 9:933274.

Becker ME, Martin-Sancho L, Simons LM, *et al*., 2024. Live imaging of airway epithelium reveals that mucociliary clearance modulates SARS-CoV-2 spread. Nature Communications 15:9480.

Bostanciklioglu M, Igci M, Ulasli M, 2024. *Nigella sativa*, *Anthemis hyaline* and *Citrus sinensis* extracts reduce SARS-CoV-2 replication by fluctuating Rho GTPase, PI3K-AKT, and MAPK/ERK pathways in HeLa-CEACAM1a cells. Gene 911:148366.

Campos-Gomez J, Fernandez Petty C, Mazur M, *et al*., 2023. Mucociliary clearance augmenting drugs block SARS-CoV-2 replication in human airway epithelial cells. American Journal of Physiology Lung Cellular and Molecular Physiology 324:L493-L506.

Cavanagh D, 2007. Coronavirus avian infectious bronchitis virus. Veterinary Research 38:281-297.

Chen C, Zuckerman DM, Brantley S, *et al*., 2014. *Sambucus nigra* extracts inhibit infectious bronchitis virus at an early point during replication. BMC Veterinary Research 10:24.

Chen H, He Y, 2022. Machine learning approaches in traditional Chinese medicine: a systematic review. American Journal of Chinese Medicine 50:91-131.

Chen H, Muhammad I, Zhang Y, *et al*., 2019. Antiviral activity against infectious bronchitis virus and bioactive components of *Hypericum perforatum* L. Frontiers in Pharmacology 10:1272.

Chen K, Gao Z, Ding Q, *et al*., 2022. Effect of natural polyphenols in Chinese herbal medicine on obesity and diabetes: interactions among gut microbiota, metabolism and immunity. Frontiers in Nutrition 9:962720.

Chen PL, Lee NY, Cia CT, *et al*., 2020. A review of treatment of coronavirus disease 2019 (COVID-19): therapeutic repurposing and unmet clinical needs. Frontiers in Pharmacology 11:584956.

Chin YF, Tang WF, Chang YH, *et al*., 2022. Orally delivered perilla (*Perilla frutescens*) leaf extract effectively inhibits SARS-CoV-2 infection in a Syrian hamster model. Journal of Food and Drug Analysis 30:252-270.

Dai QL, Jiang F, Wang J, *et al*., 2018. Based on traditional Chinese medicine inheritance support system to analyze the regularity of umbilicus application to treat ascites due to cirrhosis. Zhongguo Zhong Yao Za Zhi 43:4541-4546.

Dissook S, Umsumarng S, Mapoung S, *et al*., 2022. Luteolin-rich fraction from *Perilla frutescens* seed meal inhibits spike glycoprotein S1 of SARS-CoV-2-induced NLRP3 inflammasome lung cell inflammation via regulation of JAK1/STAT3 pathway: a potential anti-inflammatory compound against inflammation-induced long-COVID. Frontiers in Medicine 9:1072056.

Ekin S, Yildiz H, Alp HH, 2021. NOX4, MDA, IMA and oxidative DNA damage: can these parameters be used to estimate the presence and severity of OSA? Sleep Breath 25:529-536.

Feng H, Wang X, Zhang J, *et al*., 2021. Combined effect of shegandilong granule and doxycycline on immune responses and protection against avian infectious bronchitis virus in broilers. Frontiers in Veterinary Science 8:756629.

Feng H, Zhang J, Zhang K, *et al*., 2024. Synergistic anti-infectious bronchitis virus activity of phillygenin combined baicalin by modulating respiratory microbiota and improving metabolic disorders. Poultry Science 103:103371.

Ganapathy K, 2021. Infectious bronchitis virus infection of chicken: the essential role of mucosal immunity. Avian Diseases 65:619-623.

Gao P, Li X, Ding J, *et al*., 2025. Antiviral and immune enhancement effect of *Platycodon grandiflorus* in viral diseases: a potential broad-spectrum antiviral drug. Molecules 30:831.

Gul I, Hassan A, Haq E, *et al*., 2023. An investigation of the antiviral potential of phytocompounds against avian infectious bronchitis virus through template-based molecular docking and molecular dynamics simulation analysis. Viruses 15:847.

Gurung AB, Ali MA, Lee J, *et al*., 2022. Exploring the phytochemicals of *Platycodon grandiflorus* for TMPRSS2 inhibition in the search for SARS-CoV-2 entry inhibitors. Journal of King Saud University 34:102155.

Han Q, Li HH, Fan CP, *et al*., 2016. Analysis on composition principles of prescriptions for nausea by using traditional Chinese medicine inheritance support system. Zhongguo Zhong Yao Za Zhi 41:2549-2554.

Han X, Huang Y, Hao J, 2024. Avian coronavirus infectious bronchitis virus activates mitochondria-mediated apoptosis pathway and affects viral replication by inducing reactive oxygen species production in chicken HD11 cells. Biology 13:491.

He LJ, Zhu XD, 2016. Analysis on regularity of prescriptions in "a guide to clinical practice with medical record" for diarrhoea based on traditional Chinese medicine inheritance support system. Zhongguo Zhong Yao Za Zhi 41: 2344-2349.

He Y, Zheng X, Sit C, *et al*., 2012. Using association rules mining to explore pattern of Chinese medicinal formulae (prescription) in treating and preventing breast cancer recurrence and metastasis. Journal of Translational Medicine 10: S12.

Hong Q, Shang X, Wu Y, *et al*., 2023. Potential targets and mechanisms of bitter almond-licorice for COVID-19 treatment based on network pharmacology and molecular docking. Current Pharmaceutical Design 29:2655-2667.

Houeze EA, Wang Y, Zhou Q, *et al*., 2023. Comparison study of Beninese and Chinese herbal medicines in treating COVID-19. Journal of Ethnopharmacology 308:116172.

Huang B, Chen S, Wang Z, *et al*., 2025. Development and immunoprotection assessment of novel vaccines for avian infectious bronchitis virus. Virologica Sinica 40:462-476.

Ichikawa A, Kuba K, Morita M, *et al*., 2013. CXCL10-CXCR3 enhances the development of neutrophil-mediated fulminant lung injury of viral and nonviral origin. American Journal of Respiratory and Critical Care Medicine 187:65-77.

Jackwood MW, Jordan BJ, Roh HJ, *et al*., 2015. Evaluating protection against infectious bronchitis virus by clinical signs, ciliostasis, challenge virus detection, and histopathology. Avian Diseases 59:368-374.

Jiang L, An X, Duan Y, *et al*., 2022. The pathological mechanism of the COVID-19 convalescence and its treatment with traditional Chinese medicine. Frontiers in Pharmacology 13:1054312.

Jing R, Zhou J, Liu C, *et al*., 2025. Identification of a novel B cell epitope on the nucleocapsid protein of infectious bronchitis virus. International Journal of Biology and Macromolecules 330:147841.

Kumara D, Harsan HS, Septisetyani EP, *et al*., 2025. Inhibitory effects of citrus-derived flavonoids hesperidin and hesperetin on SARS-CoV-2 spike-mediated syncytia formation using *in-vitro* cell model. Advanced Pharmaceutical Bulletin 15:416-427.

Legnardi M, Tucciarone CM, Franzo G, *et al*., 2020. Infectious bronchitis virus evolution, diagnosis and control. Veterinary Science 7:79.

Li C, Wang F, Ma Y, *et al*., 2024. Investigation of the regulatory mechanisms of guiqi yimu powder on dairy cow fatty liver cells using a multi-omics approach. Frontiers in Veterinary Science 11:1475564.

Li S, 2016. Exploring traditional chinese medicine by a novel therapeutic concept of network target. Chinese Journal of Integrated Medicine 22:647-652.

Li X, Qiu Q, Li M, *et al*., 2021. Chemical composition and pharmacological mechanism of ephedra-glycyrrhiza drug pair against coronavirus disease 2019 (COVID-19). Aging 13:4811-4830.

Lillehoj H, Liu Y, Calsamiglia S, *et al*., 2018. Phytochemicals as antibiotic alternatives to promote growth and enhance host health. Veterinary Research 49:76.

Liu H, Pan S, Wang C, *et al*., 2025. Review of respiratory syndromes in poultry: pathogens, prevention and control measures. Veterinary Research 56:101.

Liu H, Wang C, He Y, *et al*., 2024. Assessing a respiratory toxic infectious bronchitis virus (IBV) strain: isolation, identification, pathogenicity, and immunological failure insights. Microbiology Spectrum 12:e0399023.

Liu J, Li D, Mei J, *et al*., 2022. Analysis of prescription and medication rules of traditional Chinese medicine in the treatment of the coronavirus disease 2019 based on traditional Chinese medicine inheritance support platform. Zhonghua Wei Zhong Bing Ji Jiu Yi Xue 34:454-458.

Lu K, Li C, Men J, *et al*., 2024. Traditional Chinese medicine to improve immune imbalance of asthma: focus on the adjustment of gut microbiota. Frontiers in Microbiology 15:1409128.

Luo W, Ding R, Guo X, *et al*., 2022. Clinical data mining reveals gancao-banxia as a potential herbal pair against moderate COVID-19 by dual binding to IL-6/STAT3. Computational Biology of Medicine 145:105457.

Ma A, Xie S, Xie H, 2025. Clinical application of Chinese herbal medicine in small animal practice. Veterinary Clinics of North America: Small Animal Practice 55:941-962.

Ma J, Huo XQ, Chen X, *et al*., 2020. Study on screening potential traditional Chinese medicines against 2019-nCoV based on Mpro and PLP. Zhongguo Zhong Yao Za Zhi 45:1219-1224.

Mikami Y, Grubb BR, Rogers TD, *et al*., 2023. Chronic airway epithelial hypoxia exacerbates injury in muco-obstructive lung disease through mucus hyperconcentration. Science Translational Medicine 15:eabo7728.

Mohajer Shojai T, Ghalyanchi Langeroudi A, Karimi V, *et al*., 2016. The effect of *Allium sativum* (garlic) extract on infectious bronchitis virus in specific pathogen free embryonic egg. Avicenna Journal of Phytomedicine 6:458-267.

Moratin H, Lang J, Picker MS, *et al*., 2025. The impact of NO2 on epithelial barrier integrity of a primary cell-based air-liquid interface model of the nasal respiratory epithelium. Journal of Applied Toxicology 45:482-491.

Najimudeen SM, Abd-Elsalam RM, Ranaweera HA, *et al*., 2023. Replication of infectious bronchitis virus (IBV) Delmarva (DMV)/1639 variant in primary and secondary lymphoid organs leads to immunosuppression in chickens. Virology 587:109852.

Nefedova E, Koptev V, Bobikova AS, *et al*., 2021. The infectious bronchitis coronavirus pneumonia model presenting a novel insight for the SARS-CoV-2 dissemination route. Veterinary Science 8:239.

Okino CH, Mores MA, Trevisol IM, *et al*., 2017. Early immune responses and development of pathogenesis of avian infectious bronchitis viruses with different virulence profiles. PLoS One 12:e0172275.

Polis B, Samson AO, 2024. Addressing the discrepancies between animal models and human Alzheimer's disease pathology: implications for translational research. Journal of Alzheimer's Diseases 98:1199-1218.

Prajapati K, Mishra R, Jain V, 2026. A comprehensive review of *Glycyrrhiza glabra* in the management of rheumatoid arthritis: ethnopharmacology, pharmacological mechanisms and synergistic therapeutic strategies. Journal of Ethnopharmacology 356:120827.

Prajapati SK, Malaiya A, Mishra G, *et al*., 2022. An exhaustive comprehension of the role of herbal medicines in pre- and post-COVID manifestations. Journal of Ethnopharmacology 296:115420.

Quinteros JA, Noormohammadi AH, Lee SW, *et al*., 2022. Genomics and pathogenesis of the avian coronavirus infectious bronchitis virus. Australian Veterinary Journal 100:496-512.

Rafique S, Jabeen Z, Pervaiz T, *et al*., 2024. Avian infectious bronchitis virus (AIBV) review by continent. Frontiers in Cellular and Infectious Microbiology 14:1325346.

Ren X, Guo Y, Wang H, *et al*., 2023. The intelligent experience inheritance system for traditional Chinese medicine. Journal of Evidence Based Medicine 16:91-100.

Najimudeen M, Shahnas, Hassan M S H, Cork S C, Abdul-Careem M F, 2020. Infectious bronchitis coronavirus infection in chickens: multiple system disease with immune suppression. Pathogens 9(10):779.

Sadeghi Dousari A, Karimian Amroabadi M, Soofi Neyestani Z, *et al*., 2023. The use of Ephedra herbs in the treatment of COVID-19. Avicenna Journal of Phytomedicine 13:231-239.

Sasse S, Arrizabalaga-Larranaga A, Sterk SS, 2024. Antiviral drugs in animal-derived matrices: a review. Heliyon 10:e37460.

Schlittenlacher T, Knubben-Schweizer G, Dal Cero M, *et al*., 2022. What can we learn from past and recent Bavarian knowledge for the future development of European veterinary herbal medicine? An ethnoveterinary study. Journal of Ethnopharmacology 288:114933.

Shu Z, Zhou Y, Chang K, *et al*., 2020. Clinical features and the traditional Chinese medicine therapeutic characteristics of 293 COVID-19 inpatient cases. Frontiers in Medicine 14:760-775.

Su KL, Xiong XJ, 2021. Treatment strategy and thought on classical herbal formulae for coronavirus disease 2019. Zhongguo Zhong Yao Za Zhi 46: 494-503.

Suhail SM, Isham IM, Farooq M, *et al*., 2025. Regulatory T cell infiltration precedes early events associated with persistent infectious bronchitis virus (IBV) infection in the cecal tonsils of chickens. Virology 612:110691.

Sultan HA, Ali A, El Feil WK, *et al*., 2019. Protective efficacy of different live attenuated infectious bronchitis virus vaccination regimes against challenge with IBV variant-2 circulating in the middle east. Frontiers in Veterinary Science 6:341.

Sun X, Wang Z, Shao C, *et al*., 2021. Analysis of chicken macrophage functions and gene expressions following infectious bronchitis virus M41 infection. Veterinary Research 52:14.

Sun X, Xu S, Liu T, *et al*., 2024. Zinc supplementation alleviates oxidative stress to inhibit chronic gastritis via the ROS/NF-kappaB pathway in a mouse model. Food Functions 15:7136-7147.

Sun Y, Niu L, Song M, *et al*., 2014. Screening compounds of Chinese medicinal herbs anti-Marek's disease virus. Pharmaceutical Biology 52:841-847.

Sun ZX, Zhang PP, Gao WL, *et al*., 2017. Analysis on medication rules of modern traditional Chinese medicines in treating palpitations based on traditional Chinese medicine inheritance support system. Zhongguo Zhong Yao Za Zhi 42:385-389.

Tamaoki J, Kondo M, Tagaya E, *et al*., 1996. Zizyphi fructus, a constituent of antiasthmatic herbal medicine, stimulates airway epithelial ciliary motility through nitric oxide generation. Experimental Lung Research 22:255-266.

Tang WF, Tsai HP, Chang YH, *et al*., 2021. Perilla (*Perilla frutescens*) leaf extract inhibits SARS-CoV-2 via direct virus inactivation. Biomedicine Journal 44:293-303.

Tian D, Chen W, Xu D, *et al*., 2024. A review of traditional Chinese medicine diagnosis using machine learning: inspection, auscultation-olfaction, inquiry, and palpation. Computational Biology of Medicine 170:108074.

Tian G, Huang C, Li Z, *et al*., 2023. Baicalin mitigates nephropathogenic infectious bronchitis virus infection-induced spleen injury via modulation of mitophagy and macrophage polarization in Hy-Line chick. Veterinary Microbiology 286:109891.

Tie Y, Liu H, Zhang T, *et al*., 2025. Natural products alleviate viral pneumonia by modulating inflammatory and oxidative-stress pathways. Frontiers in Pharmacology 16:1657829.

Wang A, Li Y, Zhao F, *et al*., 2025. Cardioprotective effect of licorice extract against myocardial ischemia and ischemia/reperfusion injury via blocking cardiac inflammation by Sirt3/NLRP3. Phytotherapy Research 39:5198-5221.

Wang B, Liu Y, Xiehe S, *et al*., 2023. Four patterns of canine wei syndrome treated with traditional Chinese medicine. Complementary Medicine Research 30:174-180.

Wang B, Zhou RR, Tang SH, 2018. Study on relevance mining of "core drug action target" in dictionary of traditional Chinese medicine prescriptions. Zhongguo Zhong Yao Za Zhi 43:3919-3926.

Wang S, 2023. Acupoint selection rules of staging, syndrome types, and symptoms of acupuncture for peripheral facial paralysis based on data mining. Zhongguo Zhen Jiu 43:1457-1464.

Wang WJ, Chen Y, Su WC, *et al*., 2022. Peimine inhibits variants of SARS-CoV-2 cell entry via blocking the interaction between viral spike protein and ACE2. Journal of Food Biochemistry 46:e14354.

Wang X, Wu S, Guo N, *et al*., 2025. *Scutellaria baicalensis* stem and leaf combat chicken-derived respiratory bacterial infection. Microbial Pathogenesis 202: 107439.

Wang X, Zhang Y, Shi L, *et al*., 2025. *Glycyrrhiza uralensis* fisch. attenuates Dioscorea bulbifera L.-induced liver injury by regulating the FXR/Nrf2-BAs-related proteins and intestinal microbiota. Journal of Ethnopharmacology 341:119319.

Wang Y, Long L, Chen M, Li J, 2025. Oxidative stress mediated by the NOX2/ROS/NF-kappaB signaling axis is involved in rosacea. Archive of Dermatology Research 317:505.

Wang Y, Xiao Q, Liu C, *et al*., 2026. Supramolecular self-assembly in traditional Chinese medicine: molecular mechanisms, material basis of decoction efficacy, compatibility interpretation, and biomedical applications. Chinese Medicine 21:36.

Wen R, Huang X, Long J, *et al*., 2024. Advances in traditional Chinese herbal medicine and their pharmacodynamic mechanisms in cancer immunoregulation: a narrative review. Translational Cancer Research 13:1166-1187.

Wu H, Wang Y, Huang J, *et al*., 2023. Rutin ameliorates gout via reducing XOD activity, inhibiting ROS production and NLRP3 inflammasome activation in quail. Biomed Pharmacotherapy 158:114175.

Wu L, Ma T, Zang C, *et al*., 2025. Glycyrrhiza, a commonly used medicinal herb: review of species classification, pharmacology, active ingredient biosynthesis, and synthetic biology. Journal of Advanced Research 75:249-270.

Xiang X, Huang Y, Li M, *et al*., 2026. Herbal treatment of IBV-*E. coli* salpingitis establishment of a salpingitis model of layer chickens caused by co-infection of infectious bronchitis virus and Escherichia coli for the curative efficacy assessment of three Chinese herbal compounds. Poult Science 105:106093.

Xiong X, Wang P, Su K, *et al*., 2020. Chinese herbal medicine for coronavirus disease 2019: a systematic review and meta-analysis. Pharmacology Research 160:105056.

Yang R, Liu H, Bai C, *et al*., 2020. Chemical composition and pharmacological mechanism of qingfei paidu decoction and ma xing shi gan decoction against coronavirus disease 2019 (COVID-19): *in-silico* and experimental study. Pharmacology Research 157:104820.

Yang X, Li J, Liu H, *et al*., 2018. Induction of innate immune response following introduction of infectious bronchitis virus (IBV) in the trachea and renal tissues of chickens. Microbial Pathogenesis 116:54-61.

Yu C, Li Y, Li Y, *et al*., 2024. A novel mechanism for regulating lung immune homeostasis: zukamu granules alleviated acute lung injury in mice by inhibiting NLRP3 inflammasome activation and regulating Th17/Treg cytokine balance. Journal of Ethnopharmacology 324:117831.

Yu X, Zhang Y, Wu B, *et al*., 2025. Multimolecular interactions from Chinese medicines activate nuclear receptor conformational changes: a potential strategy for anti-inflammatory therapy. Drug Metabolism Reviews 57:535-558.

Yurdakok-Dikmen B, Turgut Y, Filazi A, 2018. Herbal bioenhancers in veterinary phytomedicine. Frontiers in Veterinary Science 5:249.

Zhang QH, Huang HZ, Qiu M, *et al*., 2021. Traditional uses, pharmacological effects, and molecular mechanisms of licorice in potential therapy of COVID-19. Frontiers in Pharmacology 12:719758.

Zhang W, Liu Y, Zhang Q, *et al*., 2020. *Mycoplasma gallisepticum* infection impaired the structural integrity and immune function of bursa of Fabricius in chicken: implication of oxidative stress and apoptosis. Frontiers in Veterinary Science 7:225.

Zhang X, Liao K, Chen S, *et al*., 2020. Evaluation of the reproductive system development and egg-laying performance of hens infected with TW I-type infectious bronchitis virus. Veterinary Research 51:95.

Zhang XF, Yang JL, Chen J, *et al*., 2017. Optimization of a decoction process for an herbal formula using a response surface methodology. J AOAC International 100:1776-1784.

Zhang Y, Hou J, Zeng Z, 2022. Analysis of prescription medication rules of traditional Chinese medicine for diabetes treatment based on data mining. Journal of Healthcare Engineering 2022:7653765.

Zhang Y, Li XY, Zhang BS, *et al*., 2022. *In-vivo* antiviral effect of plant essential oils against avian infectious bronchitis virus. BMC Veterinary Research 18:90.

Zhang Y, Xu Z, Cao Y, 2021. Host antiviral responses against avian infectious bronchitis virus (IBV): focus on innate immunity. Viruses 13:1698.

Zhang YS, Cong WH, Zhang JJ, *et al*., 2020. Research progress of intervention of Chinese herbal medicine and its active components on human coronavirus. Zhongguo Zhong Yao Za Zhi 45:1263-1271.

Zhao J, Zhang P, Gao G, 2022. Study on intelligent traditional Chinese medicine fumigation for treating lumbar intervertebral disc herniation based on medical big data mining. Contrast Media and Molecular Imaging 2022:4658192.

Zhao J, Zhao Y, Zhang G, 2023. Key aspects of coronavirus avian infectious bronchitis virus. Pathogens 12:698.

Zhao YQ, Teng J, 2015. Analysis on composition and medication regularities of prescriptions treating hypochondriac pain based on traditional Chinese medicine inheritance support system inheritance support platform. Zhongguo Zhong Yao Za Zhi 40:1203-1206.

Zheng S, Wang Q, Qi W, *et al*., 2025. The role of Chinese medicine in the treatment of chronic hepatitis B. American Journal of Chinese Medicne 53:1285-1307.

Zhou BW, Liu HM, Jia XH, 2022. The role and mechanisms of traditional Chinese medicine for airway inflammation and remodeling in asthma: overview and progress. Frontiers in Pharmacology 13:917256.

Zhou-Suckow Z, Duerr J, Hagner M, *et al*., 2017. Airway mucus, inflammation and remodeling: emerging links in the pathogenesis of chronic lung diseases. Cell and Tissue Research 367:537-550.

Zhu H, Zhao Y, Wang X, *et al*., 2021. Research on data analysis of traditional Chinese medicine with improved differential evolution clustering algorithm. Journal of Healthcare Engineering 2021:4468741.

Zuo T, Fan XS, Tian S, *et al*., 2015. Clinical study on aconite prescriptions with incompatible herbs in different areas based on association rules and analysis on compatibility features. Zhongguo Zhong Yao Za Zhi 40:1198-1202.